

Development of Natural Product-Derived Receptor Tyrosine Kinase Inhibitors Based on Conservation of Protein Domain Fold

Lars Kissau,[†] Petra Stahl,^{†,§} Ralph Mazitschek,[‡] Athannasios Giannis,^{*,‡} and Herbert Waldmann^{*,†}

Max-Planck-Institut für molekulare Physiologie, Abteilung Chemische Biologie, Otto-Hahn-Strasse 11, 44227 Dortmund, Germany and Universität Dortmund, Fachbereich 3, Organische Chemie, 44221 Dortmund, Germany, and Institut für Organische Chemie, Universität Leipzig, Johannisallee 29, 04103 Leipzig, Germany

Received January 31, 2003

Receptor tyrosine kinases (RTKs) such as Tie-2, IGF1R, Her-2/Neu, EGFR, and VEGFR1-3 play crucial roles in the control of cell growth and differentiation. Inhibition of such RTKs has become a major focus of current anticancer drug development, and therefore the discovery of new classes of inhibitors for these signal-transducing proteins is of prime importance. We have recently proposed a novel concept for improving the hit-finding process by employing natural products as biologically validated starting points in structural space for compound library development. In this concept, natural products are regarded as evolutionary chosen ligands for protein domains which are structurally conserved yet genetically mobile. Here we report on the discovery of novel and highly selective VEGFR-2 and -3, Tie-2, and IGF1R inhibitors derived from the naturally occurring Her-2/Neu kinase inhibitor nakijiquinone C and developed on the basis of this concept. Based on the structure of the natural product, a small library (74 members) was synthesized and investigated for inhibition of kinases with highly similar ATP-binding domains. The library yielded inhibitors with IC₅₀s in the low micromolar range with high frequency (7 out of 74). In particular, four inhibitors of Tie-2 were found, a kinase critically involved in the formation of new blood vessels from preexisting ones (angiogenesis) and believed to be a new promising target in antitumor therapy. These results support the “domain concept”. To advance the development of improved inhibitors, extensive molecular modeling studies were undertaken, including the construction of new homology models for VEGFR-2 and Tie-2. These studies revealed residues in the kinase structure which are crucial to the development of tailor-made receptor tyrosine kinase inhibitors.

Introduction

Receptor tyrosine kinases play crucial roles in the transduction of signals across the plasma membrane.¹ For instance, angiogenesis, the development of new blood vessels from preexisting ones, depends on endothelium specific receptor tyrosine kinases, in particular the vascular endothelial growth factor receptors (VEGFR1-3) and the Tie-2 receptor.² All VEGFRs and Tie-2 have been implicated in tumor angiogenesis,^{3–7} and aberrant angiogenesis is considered as a key step in tumor growth, invasion, and metastasis.^{8,9}

The insulin-like growth-factor 1 receptor (IGF1R) exerts mitogenic, cell survival, and insulin-like activities, is involved in postnatal growth physiology, and is connected to proliferative disorders such as breast cancer.¹⁰ The Her-2/Neu protooncogene belongs to the EGF-family of receptor tyrosine kinases. It is overexpressed in approximately 30% of all primary breast, ovary, and stomach cancers.¹¹ The EGFR (epidermal growth factor receptor, ErbB-1) has been implicated in human tumorigenesis, for example, of glioblastoma as

well as in numerous tumors of epithelial origin including breast and oesophageal tumors.¹²

Given their biological relevance, RTKs are among the most important drug targets, and several RTK inhibitors are in advanced stages of clinical investigation or have already reached the market.^{13,14} Therefore, the development of new classes of RTK inhibitors which may be employed as tools in biological studies or as new guiding structures for the development of drug candidates is of paramount importance to clinical biology and medicinal chemistry.

We have advertised a novel concept for enhancing the efficiency of the hit-finding process.¹⁵ Within this concept, biologically active natural products that bind to structurally conserved yet genetically mobile protein domains are regarded as evolutionary selected and biologically validated starting points in structural space for compound library development. Because of their biological prevalidation and the structural conservatism employed by Nature in the repeated use of a limited number of protein domains with very similar structure, compound libraries designed on the basis of a given natural product should yield better hits at a higher rate than classical compound libraries designed on the basis of chemical accessibility alone.

In this paper we provide proof of this concept, employing the naturally occurring receptor tyrosine kinase inhibitor nakijiquinone C **1c** as a representative example.¹⁶ Nakijiquinones C and D were isolated by

* Corresponding authors. H.W.: Phone: 49-231-133-2400, Fax: 49-231-133-2499. E-mail: herbert.waldmann@mpi-dortmund.mpg.de. A.G.: E-mail: giannis@chemie.uni-leipzig.de.

[†] Max-Planck-Institut für Molekulare Physiologie and Universität Dortmund.

[‡] Universität Leipzig.

[§] Present address: Aventis Pharma AG, Chemical Research, Building G 838, 65926 Frankfurt am Main, Germany.

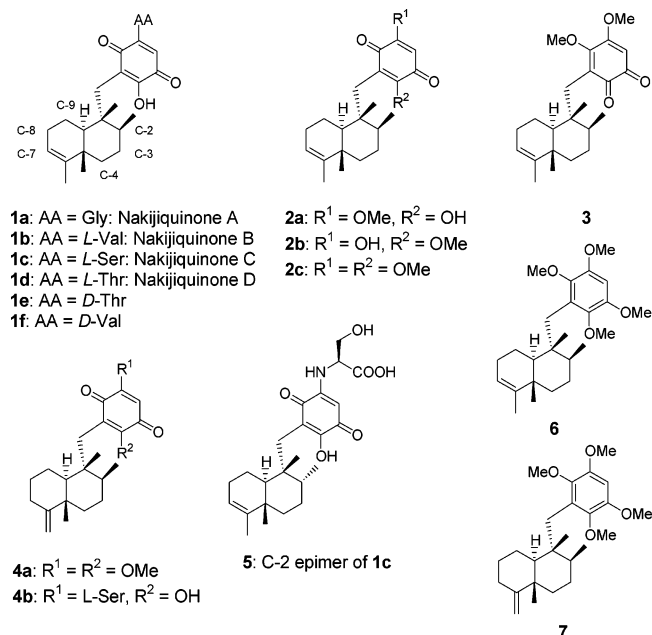


Figure 1. Structures of the nakijiquinones and structurally closely related analogues.

J. Kobayashi et al. from a marine sponge and subsequently shown to exhibit inhibitory activity against EGFR, c-erbB2, and PKC as well as cytotoxic activity against L1210 and KB tumor cell lines.¹⁷ Notably, nakijiquinone C is the first naturally occurring inhibitor of the Her-2/Neu receptor tyrosine kinase.

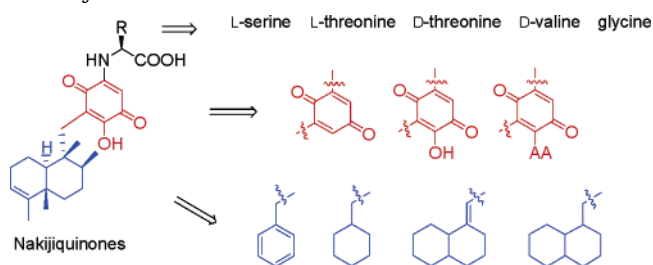
Results

For the synthesis of a nakijiquinone analogue library, initially a solid-phase approach was considered. Attachment to the solid support via the amino acid part of the molecule appeared to be advantageous for variation of the diterpene, the quinoid, and the amino acid parts of the parent compound. Unfortunately, the bond between the amino acid and the quinone is very base labile, a fact learned from initial failures encountered in the synthesis of the natural product itself.¹⁸ Thus, we proceeded to construct a library via solution-phase synthesis. The general design of the library of nakijiquinones analogues was guided by the modular composition of these natural products.

In the first series of compounds, analogues were prepared whose structure closely resembles the nakijiquinones (Figure 1). Thus, the decalin core was not changed entirely, but modified and analogues with altered configuration at C-2 and with an exocyclic double bond instead of an endocyclic one were synthesized. Also, different amino acids were introduced, or omitted, and finally the *p*-quinoid system was replaced by an *o*-quinoid structure or an aromatic group. Representative members of this library which were subsequently evaluated for biological activity are shown in Figure 1. In total 18 compounds (including nakijiquinones C and D) were prepared.¹⁸

In the second series of analogues (Scheme 1), the deviation from the natural product was more pronounced. In particular, variations were carried out on the hydrophobic diterpene unit, which according to the accepted binding mode of kinase inhibitors to the ATP-binding domain may occupy a hydrophobic pocket close

Scheme 1. Modular Composition of the Nakijiquinone Library

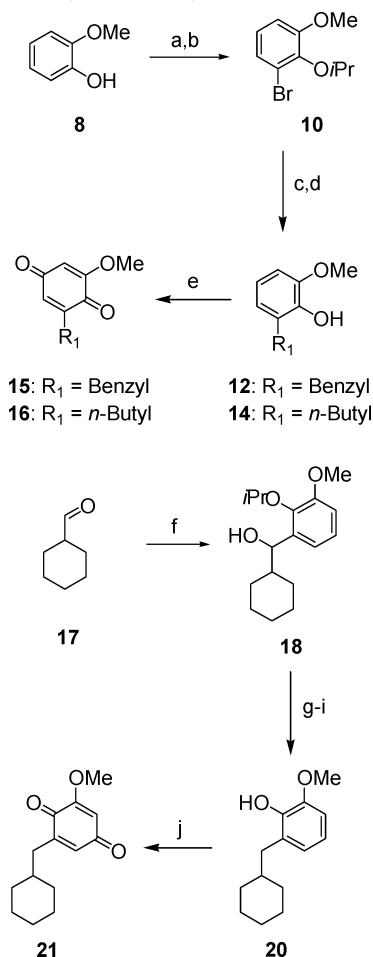


to the ATP binding site.¹⁹ Also the quinone-type building block was varied which should contribute essential hydrogen bonds to the hinge region of receptor tyrosine kinases and therefore serve to orient the inhibitor within the binding site. Finally, size and stereochemistry of the amino acid were changed, which both might enhance binding and improve selectivity via formation of hydrogen bonds and side chain interaction with the protein. Consequently, in the second series of library compounds the diterpene moiety was substituted with simple hydrophobic structures such as benzyl, *n*-butyl, and cyclohexyl groups or a *trans*-decalin. For the amino acid, the hydrophilic serine and D- and L-threonine, the hydrophobic valine, and glycine were considered. To expand the SAR data, the type and number of H-bond donors and acceptors in each library member were varied, and thus the compounds contained either one or two amino acid, hydroxyl, or methoxy groups or combinations thereof. The core *p*-quinone was left unchanged.

Commercially available guaiacol **8** was protected with 2-bromopropane and then brominated to afford compound **10**²⁰ (Scheme 2). Lithiation using *n*-BuLi and subsequent reaction with benzyl bromide yielded C-benzylated aromatic compound **11**, from which the isopropyl ether was selectively removed to give **12**. Aside from the desired lithiation and reaction with benzyl bromide, the addition of the *n*-butyl group (**13** and **14**) from *n*-BuLi was encountered. The reaction with benzyl bromide was carried out in the presence of CuI to form the cuprate. Without the addition of this copper salt, the desired coupling product was not formed.

The side reaction with *n*-BuLi could be suppressed by the use of *sec*-BuLi, but the yield of the desired benzyl-substituted quinone was not improved. Compounds **11** and **13** were not separated at this stage but immediately subjected to deprotection, employing BCl₃ to yield **12** and **14**, which could be separated. Oxidation with oxygen and salcomin²¹ as a catalyst converted these phenols to the corresponding quinones **15** and **16**.

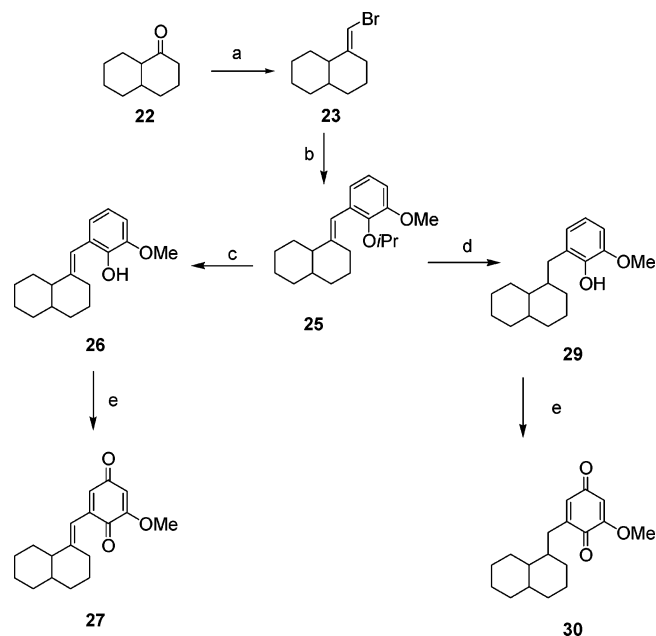
For the synthesis of compounds containing a cyclohexylmethyl substituent on the quinone, a different procedure was followed since a substitution protocol analogous to the procedure used for the benzyl analogues failed. Attempts to generate cyclohexylvinyl bromide and subject it to a Suzuki coupling with boronic acid **24**²² resulted in an unsatisfactory yield of 15%, probably due to the instability of the vinyl bromide. Thus, aryl bromide **10** was lithiated and treated with cyclohexanal **17**. The resulting alcohol **18** was converted into the corresponding oxalic acid ester **19** and deoxygenated using tributyltin hydride to give **20**.²³ After deprotection, oxidation with salcomin in DMF converted

Scheme 2. Synthesis of Nakijiquinone Analogues with Cyclohexyl, *n*-Butyl, or Benzyl Substituents^a

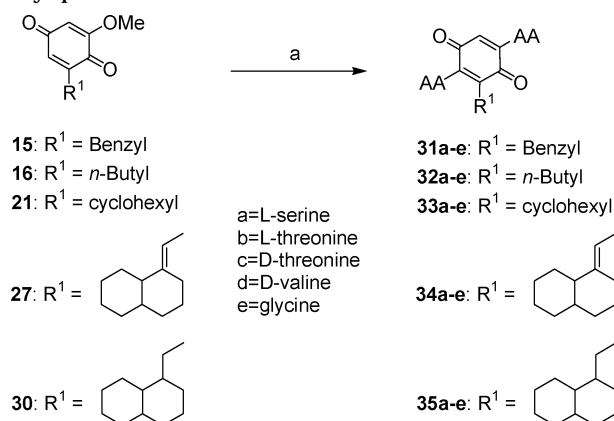
^a Reagents and conditions: (a) *i*-PrBr Yields **9** (not shown); (b) Br₂, see ref 19; (c) *n*-BuLi, THF -78 °C, CuI, R¹Br to give **11** and **13** (not shown); (d) BCl₃, CH₂Cl₂; (e) salcomine, O₂, DMF; (f) **10**, *n*-BuLi, THF, TMEDA, then **17**; (h) *i*Pr₂Net, CH₂Cl₂, methyl oxalyl chloride, DMAP; (h) toluene, AIBN, *n*-Bu₃SnH, reflux; (i) BCl₃, CH₂Cl₂; (j) salcomine, O₂, DMF.

20 into quinone **21** (Scheme 2). The deoxygenation of benzyl alcohol **18** was also feasible via conversion to the corresponding thioester followed by radical deoxygenation with tributyltin hydride and AIBN as initiator.²⁴

Finally, a *trans*-decalin was attached to the quinone core either via a CH₂ or CH bridge. Applying the established chemistry, these analogues were synthesized using again 2-hydroxy-3-methoxyphenyl bromide **9** as the starting material. Intermediate **10** was converted to boronic acid **24** which was subjected to Suzuki coupling with vinyl bromide **23** to yield olefin **25** (Scheme 3). After deprotection to give **26** oxidation yielded quinone **27**. Initial plans to synthesize **23** from *trans*-1-decalone using a Takai reaction²⁵ failed, and a Wittig reaction was employed instead. Thus, **23** was obtained in 63% yield from *trans*-1-decalone **22**. Only the (*E*)-alkene could be detected by ¹H and ¹³C NMR spectroscopy. The stereochemical assignment is based on data recorded for compounds of similar structure, for which the protons of the (*Z*)- and (*E*)-alkene differ significantly in their chemical shifts.²⁶ To obtain the methylene-bridged analogues, intermediate **25** was hydrogenated at room temperature and atmospheric

Scheme 3. Synthesis of Nakijiquinone Analogues with *trans*-Decalin Substituent^a

^a Reagents and conditions: (a) Ph₃PCH₂Br, THF, KO^tBu; (b) Pd(PPh₃)₄, **24**, EtOH, Na₂CO₃; (c) BCl₃, CH₂Cl₂; (d) MeOH, THF, Rh/Al₂O₃, H₂, to give **28** (not shown) then BCl₃, CH₂Cl₂; (e) salcomine, O₂, DMF.

Scheme 4. Synthesis of Amino Acid-Substituted Alkylquinones^a

^a Reagents and conditions: (a) amino acid, NaHCO₃, EtOH. pressure, employing a rhodium (5% supported on alumina) catalyst.²⁷

An inseparable mixture of diastereomers of **28** (3:1, determined via GC-analysis) was obtained. It was deprotected with BCl₃ to give phenol **29** (mixture of diastereomers) which was then oxidized to afford quinone **30**.

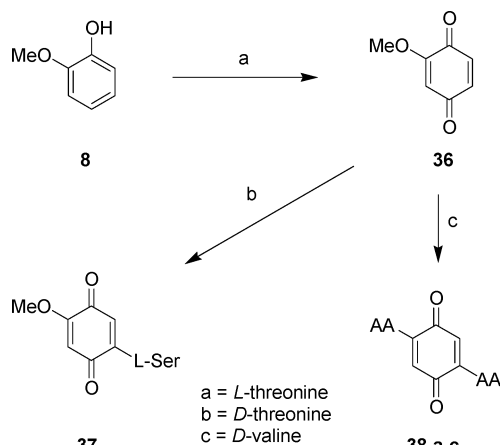
The 2-methoxy-6-alkylquinones **15**, **16**, **21**, **27**, and **30** were converted to the amino acid-substituted derivatives by stirring a solution of the quinone in ethanol in the presence of 4 equiv of NaHCO₃ and the amino acid to yield the target compounds (Scheme 4). Thus, compounds **31a-e** and **32a-e** were obtained by treatment of **15** and **16** with the corresponding amino acids. Following the same synthesis protocol, **33a-e** were synthesized from **21**, while **27** served as starting material for the synthesis of **34a-e**. Finally, **35a-e** were synthesized employing **30** as starting material (see Scheme 4).

Table 1. IC₅₀ Values (μM) of Compounds Displaying Activity toward One or More Kinases^a

compound	ErbB2	EGF	IGF1R	VEGFR-2	VEGFR-3	Tie-2
5	<i>b</i>	<i>b</i>	<i>b</i>	20 ± 3.0	<i>b</i>	<i>b</i>
15	<i>b</i>	<i>b</i>	<i>b</i>	<i>b</i>	<i>b</i>	18 ± 2.7
27	> 100	> 100	<i>b</i>	<i>b</i>	<i>b</i>	14 ± 2.1
36	29 ± 4.4	<i>b</i>	<i>b</i>	<i>b</i>	<i>b</i>	<i>b</i>
37	> 100	<i>b</i>	> 50	8 ± 1.2	<i>b</i>	<i>b</i>
38b	<i>b</i>	44 ± 6.6	6 ± 0.9	<i>b</i>	3 ± 0.5	5 ± 0.8
59c	<i>b</i>	> 100	0.5 ± 0.015	> 50	<i>b</i>	9 ± 1.4

^a IC₅₀ values were only determined for compounds displaying promising activity in the initial screening. ^b Compound showed no inhibition in an initial screen and was not investigated. Each value represents the mean standard deviation of four independent reading points.

Scheme 5. Synthesis of Nakijiquinone Analogues, Lacking an Alkyl Substituent^a



^a Reagents and conditions: (a) salcomine, O₂, DMF; (b) L-Ser, EtOH, NaHCO₃; (c) amino acid, EtOH, NaHCO₃.

The introduction of the amino acid at the C-2 position probably proceeds via an addition/elimination mechanism, while attachment of the second amino acid involves a 1,4 addition at C-6 followed by an oxidation. Since these reactions were carried out under an argon atmosphere, the quinone itself is believed to be the oxidant. This also explains the moderate yields determined for some of these conversions. In most cases, the diastereomers resulting from the reduction of the C=C double bond with Rh/Al₂O₃ could not be separated. However, the diastereomers of compound **35b** could be separated via reversed phase HPLC. Analogues lacking an alkyl substituent on the quinone were synthesized starting from commercially available guaiacol **8** (Scheme 5). The reaction sequence of oxidation to **36** and subsequent conversion to **37** and **38 a-c** followed the established protocol of stirring the quinone with the desired amino acid in ethanol in the presence of excess NaHCO₃.

For analogues of the natural products carrying one amino acid substituent and a hydroxyl group on the quinone, a different synthetic route was applied (Scheme 6). The commercially available catechol **39** was mono-protected as isopropyl ether to give **40**. After bromination of **40** ortho to the hydroxyl group to yield **41**,²⁸ oxidation to the *p*-quinone **42** was carried out with salcomin and oxygen.

Reduction with NaBH₄ and subsequent hydroxyl protection as methyl ether (**43**) was followed either by lithiation or by conversion to the boronic acid **44** (see Experimental Section) which was converted to **45** following the methodology described above. Using the method described above, **45** was then reacted with vinyl bromide **23** to give the unsaturated compound **50**, and

after hydrogenation with Rh/Al₂O₃, compound **52** was obtained. Deprotection of **45**, **50**, and **52** was achieved with BCl₃ in methylene chloride to furnish **46**, **52**, and **53**. However, the oxidation of these phenols with salcomin proceeded with only moderate yields. We therefore evaluated other oxidation methods and, finally, found that the use of Fremy's salt (ON(SO₃K)₂) in the presence of a phase-transfer catalyst was superior.²⁹ The yield over two steps (deprotection of the isopropyl ether and oxidation) was improved to 82% in the case of compound **47**. The dimethoxyalkyl-*p*-quinones **47**, **54**, and **57** derived from **46**, **52**, and **53** via oxidation were treated with KOH in methanol/water to saponify one of the vinylogous esters. This procedure had already proven successful in the total synthesis of nakijiquinone C. Finally, compounds **48**, **55**, and **58** were reacted with the desired amino acids to yield the target compounds **49a-e**, **56a-e**, and **59a-c**, respectively.

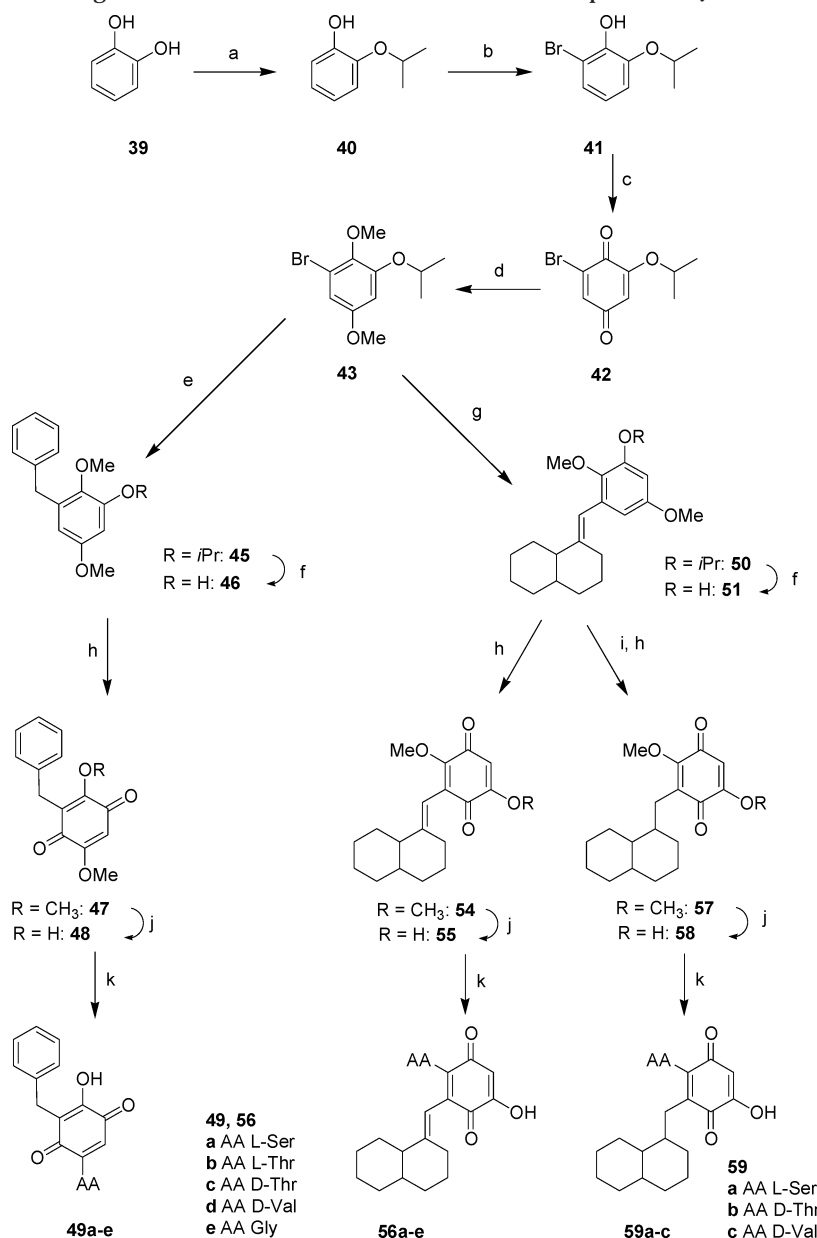
Biological Evaluation of the Library

To obtain a preliminary picture of the biochemical properties of the members of the nakijiquinone analogue library, the ability of the analogues to inhibit several different receptor tyrosine kinases were investigated. On the basis of the known biological activity of the parent nakijiquinones (see above), VEGFR-2 (KDR, flk-1), VEGFR-3 (flt-4), Tie-2, Her-2/Neu, EGFR (ErbB-1), ErbB-2, and IGF1R were chosen.

In the assay, the kinase-catalyzed phosphorylation of poly(Glu-Tyr) in the presence of varying concentrations of inhibitor was determined. The kinases were employed as fusion proteins of glutathione-S-transferase (GST) and the respective kinase domain. Kinase activity was determined by means of an anti-phosphotyrosine antibody conjugated to horseradish peroxidase (POD). The chemiluminescence caused by the reaction catalyzed by POD immobilized after antibody binding to phosphotyrosine residues was measured. Most of the library members showed no activity in this initial screen. Those compounds with noticeable inhibition, shown in Table 1, were then reevaluated in a second screening and the IC₅₀ values were determined.

Of the 74 compounds subjected to the kinase assay seven compounds displayed inhibitory activity in the low micromolar range. The library of the nakijiquinone analogues did not embody an inhibitor of Her-2/Neu, the EGFR, and ErbB-2 that warranted further detailed investigation. Most remarkably, however, four of the compounds investigated turned out to be inhibitors of the Tie-2 receptor (Table 1).

Two of these (compounds **15** and **27**) proved to be selective for this kinase, i.e., the other kinases in the assay were not inhibited more than 50% at concentra-

Scheme 6. Synthesis of Analogues with One Amino Acid and an OH Group on the Quinoid Core^a

^a Reagents and conditions: (a) *i*-PrBr, KOH, DMSO; (b) Br₂, *tert*-butylamine, toluene; (c) salcomine, O₂, DMF; (d) NaBH₄, EtOH, then (CH₃O)₂SO₂, EtOH, H₂O, NaHCO₃; (e) *n*-BuLi, THF, BnBr, CuI; (f) BCl₃, CH₂Cl₂; (g) *n*-BuLi, B(OMe)₃, to yield **44** (not shown) then **23**, Pd(PPh₃)₄, Na₂CO₃; (h) ON(SO₃K)₂ Na₂CO₃, Aliquat 336, C₆H₆, H₂O; (i) Rh/Al₂O₃, H₂, MeOH, THF, yields **52** (not shown); (j) KOH, MeOH, H₂O; (k) amino acid, NaHCO₃, EtOH.

tions up to 70 μ M. The most potent inhibitor identified in this study is **38b**. Not only does it inhibit the Tie-2 receptor with an IC₅₀ value of 5 μ M, but it is also similarly efficient in blocking the VEGFR-3 and the IGF1R. Kinetic studies revealed, that both **38b** and **59c** are ATP competitive inhibitors of the receptor tyrosine kinases evaluated.

Molecular Modeling Studies

The receptor tyrosine kinases attracting the most interest in this study as a consequence of the biological assays were Tie-2, IGF1R, VEGFR2, and VEGFR-3. Crystal structures of the kinase domains of the first three proteins have been determined; however, some of the structures show the kinases in an unliganded form. Since RTKs undergo significant structural changes upon ligand binding,¹ crystal structures without ligands are

not well suited as a basis for computer-aided ligand design. RTKs dimerize upon binding an extracellular effector followed by the phosphorylation of residues in the activation loop.¹ Since the downstream effect of the RTKs is exerted via their kinase domain, homology models of the complete kinase domains of Tie-2 and VEGFR-2 were constructed to be used in the analysis of the biological activity of the receptor tyrosine kinase inhibitors identified in this study.³⁰

The crystal structures of the FGF1 receptor³¹ were chosen as templates on the basis of the high sequence homology within the kinase domain of FGF1R with Tie-2 (~45%) and VEGFR-2 (~42%). These values are well above the 30% usually considered to be the limit for a good homology model.³² Aside from the high sequence homology, these structures contain the RTK in complex with a ligand, i.e., in an activated or closed



Figure 2. Overlay of the crystal structure of the kinase domain of insulin receptor (red) with homology models of the kinase domains for VEGFR-2 (black) and Tie-2 (yellow).³⁵

form. For model development it was assumed, that even though the Tie-2 crystal structure shows some significant structural differences to other RTKs in their unliganded forms, the conformation of the activated Tie-2 RTK, especially the ATP binding site, would be highly similar to other activated RTKs, given that the mode of ATP binding is nearly identical in these enzymes (Figure 2).³³

The importance of the “induced fit” concept and the limitations of the rigid receptor hypothesis have been discussed repeatedly.³⁴ M. Mohammadi et al. have demonstrated, that certain inhibitors cause significant changes in the conformations of loops in the kinase domain.³⁵ The two crystal structures of the FGF1 receptor containing two different types of inhibitors demonstrate the applicability of the induced fit concept to this class of enzymes. During our analysis of the nakijiquinone-type RTK inhibitors, it was found that applying this knowledge to our modeling studies resulted in improved binding modes and superior explanations for the experimental SAR data.¹⁶

Thus, for the construction of the homology models of VEGFR-2 and Tie-2, both FGF 1 receptor structures were used as templates. We believe that these homology models will be useful in the design of inhibitors, the

choice of model depending to a certain extent on the lead structure used. Our work further suggests that the exact conformation of the nucleotide binding loop of Tie-2, VEGFR-2, and IGF1R depends partially on the shape and size of the bound inhibitor, a result similar to the phenomenon described for the FGF1 receptor in complex with different inhibitors. To design high affinity ligands, it is advantageous to build different models and evaluate the interaction of a given inhibitor with each structure. Parallel to the variability of the nucleotide binding loop, the activation loop, another highly flexible region, must be scrutinized as well. Especially the position of the amino acids in the vicinity of the conserved DFG motif may be crucial for selective ligand binding. As evidenced by an overlay of several kinase structures, the exact position of the so-called C-helix varies considerably. This flexibility must also be taken into account when rationalizing experimental results or designing novel inhibitors.

The amino acid sequences for Tie-2 and VEGFR-2 were retrieved from the Swissprot Database. The primary accession numbers are P35968 (VEGFR-2) and Q02763 (Tie-2). The alignment used in the construction of these homology models was initially generated using DIALIGN³⁶ and manually corrected during the process of optimizing the models. To determine the final alignment, the highly conserved residues in the G-rich loop as well as the HRDLAARN motif were considered fixed, and the amino acids between these fixed points were shifted to yield a maximum identity or similarity. Sequence gaps were positioned in alternative positions and the resulting 3D models evaluated. The 3D model was generated using MODELLER,³⁷ a computer program that models protein 3D structure by satisfaction of spatial restraints. Using this software and a template structure with more than 40% sequence identity to the target protein, the model is likely to have about 90% of the main-chain atoms modeled with an RMS deviation from the X-ray structure of 1 Å.³⁸ The positions shown in Figure 3 gave the best results. During the optimization work, the routines implemented in the WHATCHECK software³⁹ were employed to analyze the structures generated. The structures were subse-

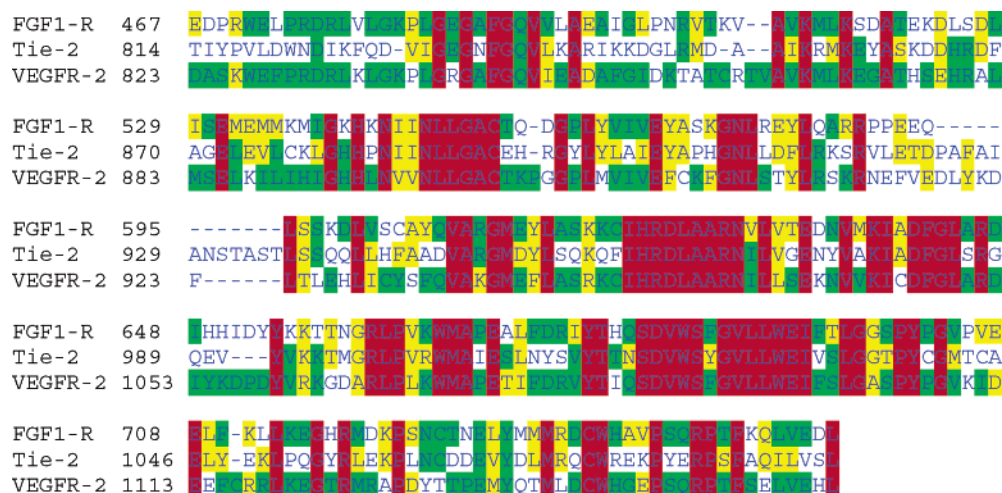


Figure 3. Alignment of the primary sequences of FGF1-R, Tie-2 (TEK), and VEGFR-2 (KDR).⁴² Identical residues are shown in green; similarity is indicated by yellow color. Consensus sequence is indicated by red background color. Figure 3 was created using BOXSHADE with the interface provided at <http://www-bioweb.pasteur.fr/seqanal/interfaces/boxshade.html>.

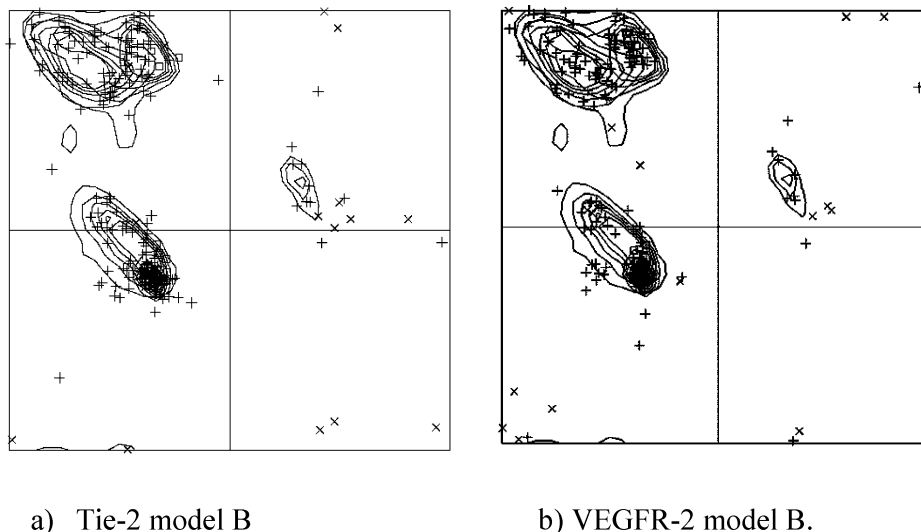


Figure 4. Ramachandran plots: (a) Tie-2 model B. (b) VEGFR-2 model B.

quently imported into WitnotP.⁴⁰ Residues in highly unlikely conformations were adjusted and all hydrogens added. For further work, the residues of the kinase insert domain were deleted from the structures since their alignment was rather poor and their influence on the design of ATP competitive inhibitors is believed to be minimal. The C-termini were changed to the *N*-methylamides, and acetamides were added to the N-termini. The resulting structures were subjected to a CHARMM⁴¹ minimization, keeping the positions of the backbone atoms fixed.

Full minimization of the proteins with no restraints resulted in a collapse of the ATP binding site if no inhibitor was present. It was thus chosen to employ the structures resulting from the minimization of side chains for the initial manual docking work. During the final minimization of the protein–ligand complexes, remaining bond and angle deviations were fixed.

The exact structures of the kinase insert domains were not predicted accurately by MODELLER, as these regions usually resulted in a random coil and unlikely ψ – ψ combinations. Since our models were intended to be employed in the design of competitive inhibitors of ATP, this region of the protein was deleted from the models to remove any unwanted strain on the position of important residues. The Ramachandran plots of the FGF1R-derived homology models are shown in Figure 4. More than 95% of the residues are found in allowed regions of the plots. The nonglycine residues found outside expected areas belong to the activation loop or highly flexible regions which are disordered in most crystal structures. None of the residues which we have termed important for the design of selective inhibitors is found outside allowed regions, however. Aside from the DFG motif, the conformation of which we believe to be correct, the prediction of the conformation of the activation loop cannot be satisfactorily achieved by the methods employed. No further optimization of this loop was carried out, since the influence on the shape of the ATP binding pocket is thought to be marginal. The correct conformation of the activation loop would be required for the design of bisubstrate inhibitors. However, none of the kinase inhibitors currently under development or clinical investigation attempts to mimic

Table 2. Residue Substitutions in the Hydrophobic Pocket

residue in IGF1R	residue in VEGFR-2	residue in Tie-2
Leu 1002	Leu 840	Ile 830
Met 1076	Val 916	Ile 902
Val 1060	Val 899	Ile 886
Val 1065	Val 914	Leu 900
Phe 1054	Ile 892	Leu 879
Met 1051	Leu 889	Leu 876
Val 1050	Ile 888	Val 875
Met 1139	Leu 1035	Leu 971
Gly 1149	Cys 1045	Ala 981

the substrate, and this route does not appear to be promising.

In addition, the conformational alterations in the activation loop of kinases are manifold.¹ To assign a conformation of this loop via homology modeling would be very speculative.

In Figures 5 a–d, the side chain atoms of those residues believed to be important for achieving selectivity between kinases are displayed. An overlay of the kinase domain models provides a good basis for the design of selective inhibitors for each enzyme. Several substitutions alter the shape and size of the hydrophobic pocket and the region where the purine moiety of ATP would be bound. These substitutions are listed in Table 2.

Aside from the substitutions in the hydrophobic pocket, variations in the nucleotide binding loop cannot be disregarded. Next to the conserved phenylalanine (F835 in Tie-2, F845 in VEGFR-2, and F980 in IGF1R), A844 in VEGFR-2 is replaced by N834 in Tie-2 and S979 in IGF1R. As shown previously,¹⁷ the asparagine in Tie-2 may contribute to the hydrogen bonding to an inhibitor by Tie-2 and via this interaction favors a conformation of the nucleotide binding loop as shown in Figure 5b. This in turn may synergistically advance lipophilic interactions between the phenylalanine and the hydrophobic residues of potential inhibitors. The differences listed here provided a good explanation for the patterns of selectivity observed for nakijiquinone analogues and in the future can be exploited for fine-tuning of the selectivity of optimized RTK inhibitors.

Static homology models have their limitations with respect to being able to account for all detected struc-

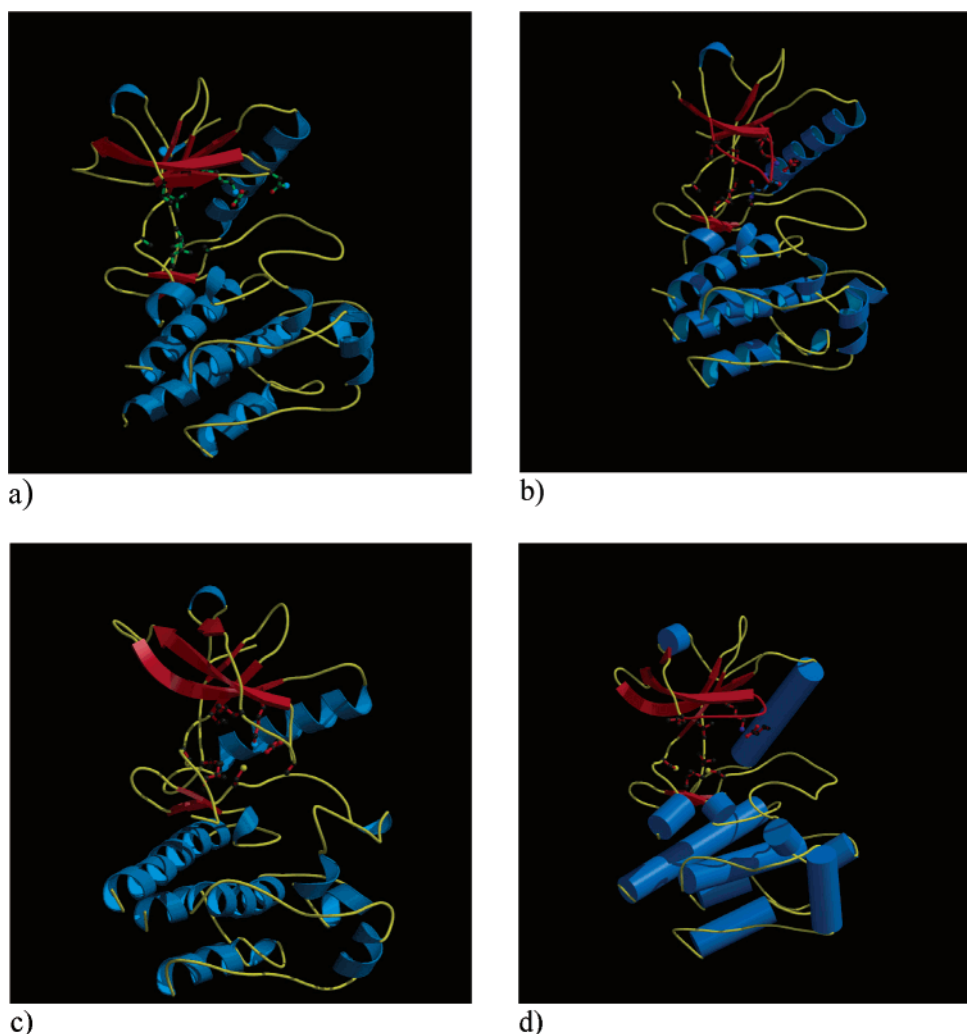


Figure 5. Developed models for Tie-2 and VEGFR-2: (a) Tie-2 model B. (b) Tie-2 model A. (c) VEGFR-2 model A. (d) VEGFR-2 model B.

tural characteristics. For instance, the role of the exchange Phe \rightarrow Tyr in the hinge region can at present not be explained. None of the known inhibitors of these kinases exhibits a marked interaction with the phenolic OH. Likewise, the full effect of the Pro at the beginning of the KDR nucleotide binding loop cannot be elucidated easily. In addition, more information from further crystal structures of these kinases in complex with inhibitors is needed to fully understand the possible *in vivo* conformations of the activation loop. Likewise, the significant motion of the C-helix can only be properly estimated by analysis of the structures in complex with inhibitors of varying morphology or by supportive experimental data.

With the completed homology models in hand, we set out to determine and explain the molecular basis for the biological activity of the nakijiquinone analogues. In addition to the previously evaluated compounds, the interactions of compounds **38b** and **59c** with VEGFR-2, Tie-2, and IGF1R were explored. The structural differences in the hydrophobic pocket as described above provided a useful rationalization for the experimental observations. The fact that VEGFR-2 is not inhibited by **59c** can be explained by a steric clash of the decalin with Cys1045, which corresponds to Ala981 and Gly1122 in Tie-2 and IGF1R, respectively. The 18-fold higher

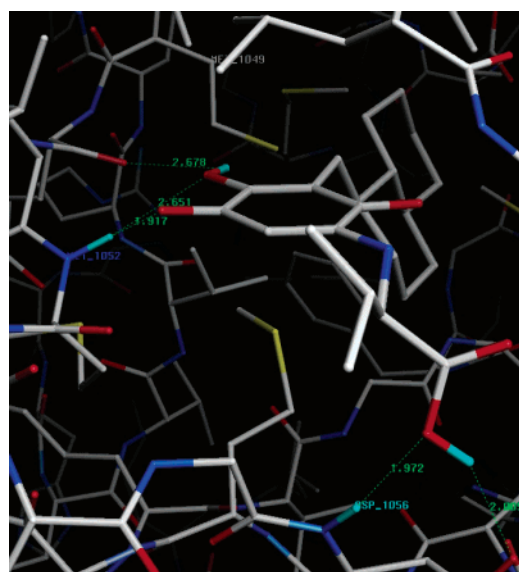


Figure 6. Proposed binding mode of **59c** to IGF1R.

inhibition of IGF1R compared to Tie-2 is, according to our analysis, caused by the stronger hydrophobic interaction of the *trans*-decalin with the (smaller) hydrophobic pocket in IGF1R. The proposed binding mode of **59c** to IGF1R is shown in Figure 6.

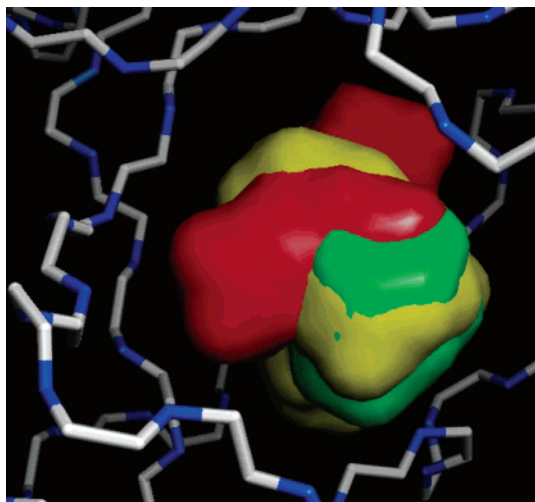


Figure 7. The solvent-accessible volume of the hydrophobic pocket of IGF1R (green), KDR (yellow), and Tie-2 (red)

We note that compound **59c** was obtained as an inseparable mixture of diastereomers whose composition could not be determined by NMR spectroscopy. Molecular modeling suggests, however, that the diastereomer depicted in Figure 6 is expected to be the active component, since the other diastereomer would not fit well into the binding site in the homology model.

This result, combined with our previously published analyses, provides a good indication about future fine-tuning of selectivity toward a particular kinase. Exploring the differences in the hydrophobic pocket, for example, by adding different substituents at varying positions of the decalin moiety, should allow the use of nakijiquinone analogues as a molecular tool kit for the study of the biological effects caused by inhibition of a certain receptor tyrosine kinase. The explanation for the selectivity of the bis-threonine derivative **38b** follows the same lines. It too is an ATP competitive inhibitor. The selectivity between VEGFR-2 and VEGFR-3 is somewhat intriguing, given their homology, especially within the ATP binding site. Further variation of this structure should provide sufficient data to fully elucidate the binding mode of receptor tyrosine kinase inhibitors belonging to this compound class.

We note, however, that the structure of **38b** does not fit the amino acid–quinone–decalin pattern displayed by **59c**. Since the positioning of a carboxylate in the hydrophobic pocket is improbable, **38b** must bind in a different mode. Our molecular modeling work indicates that a binding mode where **38b** blocks the triphosphate binding region without interacting with residues in the hinge region could serve as an explanation. Such a binding mode would provide hints to the cause of the intriguing selectivity between VEGFR-2 and VEGFR-3.

Further proof of the importance of exploiting structural differences in the hydrophobic pocket to attain selectivity can be derived from comparing the size and shape of the hydrophobic pockets in our homology models.⁴²

Figure 7 demonstrates, the possibility of achieving selectivity through variation of the hydrophobic part of an inhibitor, while leaving the part which contributes essential hydrogen bonds to the hinge region untouched.

Discussion

This article describes the synthesis of a small library of analogues of the naturally occurring tyrosine kinase inhibitor nakijiquinone C and its evaluation with respect to the inhibition of other kinases. The investigation is based on the recently proposed concept that natural products are biologically validated starting points in structural space for compound library development. Within this concept they are regarded as molecular entities selected by evolution for binding to structurally conserved yet genetically mobile protein domains. The proteins investigated in this study were chosen on one hand for their biological relevance (i.e., involvement in tumorigenesis, angiogenesis, or lymphangiogenesis) and on the other hand due to the high homology in their ATP binding kinase domains (>45%). According to the above-mentioned “domain concept”, this high homology suggests that a library synthesized around a natural product binding to such domains should yield ligands for the similar domains in other proteins with a high hit rate. An overlay of the crystal structures of FGF1R, IGF1R, and the homology models generated for VEGFR-2 and Tie-2 (similar to Figure 2) and comparison with the homology to the ATP binding domain in the natural target Her-2/Neu of the underlying nakijiquinone C (34% homology to FGF1R) suggests that a nakijiquinone-derived library should fulfill the demands raised above.

In this paper we focus on a natural product with proven biological activity as a biologically prevalidated starting point in structural space for compound library development. We would like to stress, however, that the requirement of biological prevalidation is not limited to naturally occurring compounds. Of course nonnatural compound classes that have been found to be biologically relevant can be employed as structural starting points within the reasoning of our proposal as well.

After the development of the first ATP competitive kinase inhibitors and the determination of the first kinase structure (PKA),⁴³ the successful development of selective ATP-competitive inhibitors was thought to be highly unlikely given the high degree of conservation of residues involved in ATP binding and the similarity of the kinase domains.¹³ Our work and the success encountered in the kinase field during the past decade support our proposal that the similarity of protein domains should be employed for the development of selective inhibitors based on an already biologically validated compound.

The data described above show that a relatively small library designed around a naturally occurring kinase inhibitor may yield potent inhibitors for other kinases with a high hit rate (7 inhibitors out of 74 compounds investigated). Starting from the natural product nakijiquinone C, a known inhibitor of the Her-2/Neu kinase, structurally related analogues were found to inhibit Tie-2, VEGFR2/3, and IGF1R. Several of the hits clustered at the kinase Tie-2. While from a 74-member library a statistically relevant statement cannot be deduced, this result clearly supports the validity of the domain concept for library development.

The results recorded in this study also convincingly demonstrate that the trains of thought starting from protein domains and biologically active natural products

call for the synthesis of compound libraries. The use of a given natural product alone is not sufficient. Thus, the original nakijiquinone was not active on any of the other kinases investigated.

In line with the domain concept, natural products and domain structure therefore can only be regarded as the initial starting points in the hit finding process. The varying amino acid sequences found in domains with very similar fold call for the generation of chemical diversity in the library that matches the diversity in the precise architecture of domains with conserved fold. In a sense, the similarity of protein structures provides the basis for the choice of the underlying framework of the library members, and then the differences in the similar protein structures are exploited to obtain selectivity. We would like to point out that the Tie-2 and VEGFR-3 inhibitors identified in this study might be used advantageously for the development of a new class of agents to interfere in the processes of angiogenesis (Tie-2) and lymphangiogenesis. Given its different pattern of H-bond donors/acceptors when compared to other active members of the library, this may be particularly true for the bis(threonine) derivative **38b**. At the outset of the study inhibitors of Tie-2 and VEGFR-3 were not known (in the meantime Tie-2 inhibitors were identified).^{44–49} This underscores the potential harbored by the domains/natural product approach. The inhibition of IGF1R by **59c** and its selectivity also warrant further investigation.

The similarity of the domains facilitates the use of modern methods of molecular modeling to rationalize the experimental findings and to further stimulate the development of improved inhibitors. In this context, the development of convincing homology models becomes important, in particular when extensive structural data (X-ray, NMR structures) of the domains are missing. In this study, two homology models for the receptor tyrosine kinases Tie-2 (TEK) and VEGFR-2 (KDR)⁵⁰ were developed and employed in the molecular modeling studies. In agreement with established models for RTK inhibitors, analysis of these models has shown that selective inhibitors cannot be designed by attempting to form different pattern of hydrogen bonds alone. Rather, differences in the hydrophobic pockets have to be exploited. Instead, the hydrogen bonds serve to orient the compounds within the active site. These findings are consistent with results previously reported for FGF1-R, IGF1R, and VEGFR-2.⁵¹ Furthermore, we believe these enzymes to be a convincing demonstration of the limitations of the rigid receptor hypothesis. Rather than fitting molecules into a rigid receptor structure, it appears to be crucial to build several models to accommodate inhibitors of varying shapes and sizes. Finally, we have employed these models to elucidate the SAR data collected from our nakijiquinone analogue library. These results can now be employed for the design of more active and selective inhibitors of the receptor tyrosine kinases Tie-2 and VEGFR-2.

Experimental Section

General. Melting points were determined in open capillaries using a Büchi 535 apparatus and are uncorrected. ¹H and ¹³C NMR spectra were recorded on a Bruker AC 250 or DRX 500 spectrometer at room temperature. IR spectra were recorded on a Bruker IFS 88 spectrometer. Mass spectra and

high-resolution mass spectra (HRMS) were measured on a Finnigan MAT MS70 (for EI and FAB) or a Finnigan LCQ (for ESI, all samples are solved in H₂O/MeOH/5%HCOOH) spectrometer. Specific rotations were measured with a Perkin-Elmer 241 polarimeter. Flash chromatography was performed using Baker silica gel (230–400 mesh ASTM). Reaction progress was monitored by TLC using Merck silica gel 60F254 aluminum sheets (Merck, Darmstadt, Germany).

High-pressure liquid chromatography (HPLC) was performed with a Rainin-Dynamax (model SD-300) instrument. A gradient composed of I (0.1% TFA in water) and II (0.1%TFA in acetonitrile) was used for semipreparative and preparative HPLC; method A: Time 0, 20% II. Time 15 min 40% II. Time 30 min 100% II. Time 35 100% II. Method B: Time 0, 50% II. Time 15 min 75% II. Time 30 min 100% II. Time 35 100% II.

Molecular Modeling. The molecular modeling studies were carried out on a SGI O2 work station (RS10000, 300 MHz). The CHARMM version used for the minimizations of protein–ligand complexes was c27b. Input files for CHARMM were created within WitnotP. Minimizations were performed on an Origin 2000 (16 x RS12000 400 MHz). The homology models were constructed using MODELLER version 4.0, using the standard settings. The Ramachandran plots of the homology models were created using WHATCHECK. The volumes and shapes of the hydrophobic pocket were calculated by filling the voids using the PASS algorithm. The front boundary was arbitrarily defined by a plane constructed using F1007-C α , F1007-C, M1076-C α , and M1076-N (numbers referring to the IGF1R sequence) and the corresponding residues in VEGFR-2 and Tie-2. The pseudo-atoms placed by PASS were covered with an SA-surface (probe radius 1.4 Å). Volumes were calculated using WitnotP.

The homology model employed in this study differs from the model used in our previous publication.^{17c} The homology model for the VEGFR-2 active site used in the previous publication was derived by replacing corresponding residues in the FGF1R structure, neglecting all residues located more than 5 Å from the ATP binding site. To determine if differences in the primary sequences in more remote parts of the kinase domain could influence the shape and size of the ATP binding pocket, a full model based on the FGF1R template was created using MODELLER. The new model shows the nucleotide binding loop in a slightly different form than in the previous model.

3-Methoxy-2-isopropoxyphenyl Bromide (10). To 85 mL of DMSO was added KOH (8.90 g, 0.159 mol). After the mixture was stirred for 10 min, 2-hydroxy-3-methoxyphenyl bromide **9** (8.70 g, 42.9 mmol) was added, followed after 10 min by 2-bromopropane (8.1 mL, 86.3 mmol). Stirring was continued for 1 h after which the KOH was filtered and the filtrate was diluted with 100 mL CH₂Cl₂. The organic layer was washed with a saturated solution of NH₄Cl (2 \times), NaCl (2 \times), dried over Na₂SO₄, and evaporated to dryness under reduced pressure. The crude product was purified by flash chromatography on silica gel (95:5 hexane/EtOAc) to give 10.1 g (96%) of pure **4** as a colorless oil. *R*_f: 0.64 (9:1 hexane/EtOAc); ¹H NMR (250 MHz, CDCl₃): δ 7.12 (dd, ³*J* = 7.5 Hz, ⁴*J* = 2.0 Hz, 1H, H-6), 6.90–6.80 (m, 2H, H-4, H-5), 4.59–4.50 (m, 1H, CH(CH₃)₂), 3.81 (s, 3H, OCH₃), 1.32 (d, ³*J* = 6.2 Hz, 6H, CH(CH₃)₂); ¹³C NMR (62.9 MHz, CDCl₃): δ 154.1 (C-3), 144.7 (C-2), 125.0 (C-6), 124.2 (C-5), 118.7 (C-4), 111.5 (C-1), 75.8 (CH(CH₃)₂), 55.9 (OCH₃), 22.5 (CH(CH₃)₂); MS (EI, 70 eV): *m/z* (%) 246/244 (17/17) [M⁺], 204/202 (98/100) [M⁺ – C(CH₃)₂], 189/187 (29/29) [M⁺ – CH₃ – C(CH₃)₂], 124 (10), 109/107 (6/5), 79 (7); HRMS (70 eV): calcd for C₁₀H₁₃O₂⁸¹Br: 246.0079, found: 246.0076.

6-Benzyl-2-methoxyphenol (12) and 6-Butyl-2-methoxyphenol (14). To a solution of 3-methoxy-2-isopropoxyphenyl bromide **10** (300 mg, 4.90 mmol) in 3.2 mL THF at –78 °C was added dropwise *n*-BuLi (2.5 M in hexane) (539 μ L, 1.35 mmol). After the mixture was stirred at this temperature for 30 min, CuI (285 mg, 1.50 mmol) was added. The solution was slowly warmed to –40 °C, then cooled to –78 °C, and at this temperature a solution of benzyl bromide (217 μ L, 1.83 mmol) in 0.5 mL of THF was added. The mixture was warmed to room

temperature, diluted with 20 mL ether and 20 mL water, and extracted with ether (1 × 20 mL). The combined organic layers were washed with a saturated solution of Na₂CO₃ until the aqueous layer was colorless, dried over Na₂SO₄, and evaporated under reduced pressure. The crude product was purified by flash chromatography on silica gel (95:5 hexane/EtOAc) to give 111 mg of products **11** and **13** as a mixture.

To a solution of the mixture of **11** and **13** in 10 mL of CH₂Cl₂ at 0 °C was added BCl₃ (1 M in CH₂Cl₂, 510 μL, 0.51 mmol). After the mixture was stirred at 0 °C for 1 h, water was added, and the mixture was extracted with CH₂Cl₂ (3 × 15 mL). The combined organic layers were dried over Na₂SO₄ and evaporated under reduced pressure. The crude product was purified by flash chromatography on silica gel (95:5 hexane/EtOAc) to give 44.9 mg (17%, 2 steps) of pure **12** as a colorless oil and 46.8 mg (21%, 2 steps) of pure **14** as a colorless oil.

Compound 12: *R_f*: 0.54 (9:1 hexane/EtOAc); ¹H NMR (250 MHz, CDCl₃): δ 7.26–7.14 (m, 5H, H-2'(2), H-3'(2), H-4'), 6.77–6.68 (m, 3 H, H-3, H-4, H-5), 5.73 (d, ⁴*J* = 1.53 Hz, 1H, OH), 4.00 (s, 2H, H-7), 3.85 (s, 3H, OCH₃); ¹³C NMR (62.9 MHz, CDCl₃): δ 146.5 (C-2), 143.6 (C-1'), 140.9 (C-1), 129.0, 128.4, 127.1 (C-6, C-2'(2), C-3'(2)), 126.0 (C-4'), 122.9 (C-4), 119.5 (C-5), 108.8 (C-3), 56.1 (OCH₃), 35.6 (C-7); MS (EI, 70 eV): *m/z* (%) 214 (100) [M⁺], 197 (7) [M⁺ – OH], 181 (19), 153 (12), 136 (23), 107 (6), 91(5); HRMS (70 eV): calcd for C₁₄H₁₄O₂: 214.0994, found: 214.0989.

Compound 14: *R_f*: 0.6 (9:1 hexane/EtOAc); ¹H NMR (250 MHz, CDCl₃): δ 6.80–6.67 (m, 3 H, H-3, H-4, H-5), 5.68 (d, ⁴*J* = 1.83 Hz, 1H, OH), 3.82 (s, 3H, OCH₃), 2.67–2.61 (m, 2H, (CH₂CH₂CH₂CH₃)), 1.66–1.54 (m, 2H, (CH₂CH₂CH₂CH₃)), 1.45–1.28 (m, 2H, (CH₂CH₂CH₂CH₃)), 0.98–0.87 (m, 3H, (CH₂CH₂CH₂CH₃)); ¹³C NMR (62.9 MHz, CDCl₃): δ 146.2 (C-2), 143.5 (C-1), 128.8 (C-6), 122.4 (C-5), 119.2 (C-4), 108.2 (C-3), 56.0 (OCH₃), 31.8 (CH₂CH₂CH₂CH₃), 29.5 (CH₂CH₂CH₂CH₃), 23.0 (CH₂CH₂CH₂CH₃), 14.1 (CH₂CH₂CH₂CH₃); MS (EI, 70 eV): *m/z* (%) 180 (53) [M⁺], 137 (100) [M⁺ – CH₂CH₂CH₃], 106 (8) [M⁺ – CH₂CH₂CH₃ – OCH₃], 77 (7), 41 (3); HRMS (70 eV): calcd for C₁₁H₁₆O₂: 180.1150, found: 180.1118.

6-Benzyl-2-methoxy-2,5-cyclohexadiene-1,4-dione (15). To a solution of 6-benzyl-2-methoxyphenol **12** (50.9 g, 0.237 mmol) in 1.5 mL of DMF was added salcomine (*N,N*-bis(salicylidene)ethylendiamine-cobalt(II) hydrate) (8.7 mg, 26 μmol). The solution was stirred at room temperature under an oxygen atmosphere for 12 h, after which the solution was diluted with 20 mL of ether and 10 mL of water, and extracted with ether (3 × 15 mL). The combined organic layers were dried over Na₂SO₄ and evaporated under reduced pressure. The crude product was purified by flash chromatography on silica gel (4:1 hexane/EtOAc) to give 38 mg (70%) of pure **15** as a yellow solid. *R_f*: 0.26 (3:1 hexane/EtOAc); mp 127 °C; ¹H NMR (500 MHz, CDCl₃): δ 7.33–7.18 (m, 5H, H-2'(2), H-3'(2), H-4'), 6.30 (dd, ⁴*J* = 1.5 Hz, ⁴*J* = 2.3 Hz, 1H, H-5), 5.86 (d, ⁴*J* = 2.3 Hz, 1H, H-3), 3.81 (s, 3H, OCH₃), 3.75 (d, ⁴*J* = 1.5 Hz, 2H, H-7); ¹³C NMR (125.6 MHz, CDCl₃): δ 187.4 (C-1), 181.8 (C-4), 158.8 (C-2), 146.7 (C-6), 136.4 (C-1'), 133.8 (C-5), 129.4 (C-2'(2C)), 128.3 (C-3'(2C)), 127.0 (C-4'), 107.2 (C-3), 56.3 (OCH₃), 34.9 (C-7); MS (EI, 70 eV): *m/z* (%) 228 (100) [M⁺], 213 (45) [M⁺ – CH₃], 197 (5) [M⁺ – OCH₃], 196 (18), 168 (5), 157 (8), 143 (12), 128(8), 115 (34); HRMS (70 eV): calcd for C₁₄H₁₂O₃: 228.0786, found: 228.0791.

1-Cyclohexyl-4-methoxy-3-isopropoxybenzyl Alcohol (18). To a solution 3-methoxy-2-isopropoxyphenyl bromide **9** of (200 mg, 0.817 mmol) in 5.9 mL of THF was added dropwise 1.3 mL of TMEDA. The mixture was cooled to –78 °C, and *n*-BuLi (2.5 M in hexane, 2.2 mL, 5.5 mmol) was added dropwise. The solution was slowly warmed to –40 °C, then cooled to –78 °C, and to this solution was added a solution of cyclohexanecarbaldehyde **17** (316 μL, 4.10 mmol) in 3.3 mL of THF. The mixture was warmed to room temperature and diluted with 15 mL of ether. The organic layer was washed with 2 N HCl (2 × 15 mL) and brine, dried over Na₂SO₄, and evaporated under reduced pressure. The crude product was purified by flash chromatography on silica gel (95:5 hexane/

EtOAc) to give 208 mg (91%) of pure **18** as a colorless oil. *R_f*: 0.19 (9:1 hexane/EtOAc); ¹H NMR (500 MHz, CDCl₃): δ 7.04–6.91 (m, 2H, H-6, H-7), 6.81–6.77 (m, 1H, H-5), 4.74–4.71 (m, 1H, H-1), 4.65–4.55 (m, 1H, OCH(CH₃)₂), 3.83 (s, 3H, OCH₃), 3.47–3.40 (m, 1H, OH), 2.39–2.28 (m, 1H, H-1'), 2.17–0.83 (m, 10H, cyclohexane), 1.35 (d, ³*J* = 6.1 Hz, 3H, OCH(CH₃)₂), 1.22 (d, ³*J* = 6.1 Hz, 3H, OCH(CH₃)₂); ¹³C NMR (125.6 MHz, CDCl₃): δ 152.3 (C-4), 144.0 (C-3), 137.7 (C-2), 123.2 (C-7), 119.1 (C-6), 110.8 (C-5), 81.2 (C-1), 74.3/74.0 (OCH(CH₃)₂), 55.5 (OCH₃), 44.4/43.7 (C-1'), 29.4/29.3 (C-4'), 28.9/28.6 (C-3'), 26.7/26.5 (C-3'), 26.2/26.0 (C-2'), 25.7/25.5 (C-2'), 22.9/22.3 (OCH(CH₃)₂), 21.5/21.0 (OCH(CH₃)₂); MS (EI, 70 eV): *m/z* (%) 278 (11) [M⁺], 218 (7) [M⁺ – C₃H₇ – OH], 195 (24) 153 (100) [M⁺ – C₃H₇ – C₆H₁₀], 137 (14) [M⁺ – OC₃H₇ – C₆H₁₀], 93 (7); HRMS (70 eV): calcd for C₁₇H₂₆O₃: 278.1882, found: 278.1873.

1-Cyclohexyl-4-methoxy-3-isopropoxybenzylmethoxyoxalyl Ester (19). DIPEA (198.0 μL, 1.13 mmol), with a catalytic amount of DMAP, followed by methyl oxalyl chloride (104 μL, 1.13 mmol) were added to a solution of alcohol **18** (50 mg, 0.18 mmol) in dry CH₂Cl₂. The reaction mixture was stirred at room temperature for 24 h. The reaction was diluted with 10 mL of CH₂Cl₂ and washed with a saturated solution of Na₂CO₃ and brine. The water solution was extracted with CH₂Cl₂ (2 × 15 mL). The combined organic layers were dried over Na₂SO₄ and evaporated under reduced pressure. The crude product was purified by flash chromatography on silica gel (95:5 hexane/EtOAc) to give 44.4 mg (68%) of pure **19** as a colorless oil. *R_f*: 0.38 (9:1 hexane/EtOAc); ¹H NMR (500 MHz, CDCl₃): δ 7.01 (*ψ*t, ³*J* = 7.9 Hz, 1H, H-7), 6.94 (dd, ³*J* = 7.9 Hz, ⁴*J* = 1.4 Hz, 1H, H-6), 6.82 (dd, ³*J* = 8.0 Hz, ⁴*J* = 1.4 Hz, 1H, H-5), 6.18 (d, ³*J* = 7.0 Hz, 1H, H-1), 4.69–4.64 (m, 1H, OCH(CH₃)₂), 3.83 (s, 3H, OCH₃), 2.35–2.28 (m, 1H, H-1'), 1.95–0.92 (m, 10H, cyclohexane), 1.39 (d, ³*J* = 6.1 Hz, 3H, CH(CH₃)₂), 1.25 (d, ³*J* = 6.1 Hz, 3H, OCH(CH₃)₂); ¹³C NMR (125.6 MHz, CDCl₃): δ 158.6 (C=O), 157.1 (C=O), 152.4 (C-4), 144.1 (C-3), 132.8 (C-2), 123.2 (C-7), 118.7 (C-6), 111.4 (C-5), 78.4 (C-1), 74.9 (OCH(CH₃)₂), 55.5/53.4 (OCH₃), 43.6/43.1 ((CO)₂OCH₃), 41.2/41.1 (C-1'), 29.2/29.1 (C-4'), 28.8/28.3 (C-3'(2)), 26.2/26.0 (C-2'(2)), 22.9, 22.3 (OCH(CH₃)₂); MS (EI, 70 eV): *m/z* (%) 364 (12) [M⁺], 219 (16) [M⁺ – C₃H₆ – CH₃O(CO)₂O], 218 (100) [M⁺ – C₃H₇ – CH₃O(CO)₂O], 138(10), 137 (59) [M⁺ – C₃H₆ – C₆H₁₀ – CH₃O(CO)₂O]; HRMS (70 eV): calcd for C₂₀H₂₈O₆: 364.1886, found: 364.1892.

6-(Cyclohexylmethyl)-2-methoxyphenol (20). To a solution of methoxyoxalyl ester **19** (44.4 mg, 0.122 mmol) in 8.7 mL of dry toluene were added tributyltin hydride (66 μL, 0.249 mmol) and a catalytic amount of AIBN. The reaction mixture was heated at reflux for 2 h. The solvent was removed in vacuo, and the residue was purified by flash chromatography on silica gel (95:5 hexane/EtOAc). To a solution of the deoxygenated product in 6.3 mL of CH₂Cl₂ at 0 °C was added BCl₃ (1 M in CH₂Cl₂) (135 μL, 0.135 mmol). After the mixture was stirred at 0 °C for 1 h, water was added and extracted with CH₂Cl₂ (3 × 10 mL). The combined organic layers were dried over Na₂SO₄ and evaporated under reduced pressure. The crude product was purified by flash chromatography on silica gel (95:5 hexane/EtOAc) to give 9.8 mg (37%, two steps) of pure **20** as a white solid; *R_f*: 0.48 (9:1 hexane/EtOAc); mp 52 °C; ¹H NMR (500 MHz, CDCl₃): δ 6.77–6.69 (m, 3H, H-3, H-4, H-5), 5.64 (d, ⁴*J* = 3.0 Hz, 1H, OH), 3.88 (s, 3H, OCH₃), 2.55 (d, ³*J* = 7.1 Hz, 2H, H-7), 1.70–0.90 (m, 11H, cyclohexane); ¹³C NMR (125.6 MHz, CDCl₃): δ 146.3 (C-2), 143.7 (C-1), 127.2 (C-6), 123.4 (C-5), 118.8 (C-4), 108.0 (C-3), 55.9 (OCH₃), 38.2 (C-7), 37.5 (C-1'), 33.3 (C-2'(2)), 26.6 (C-4'), 26.4 (C-3'(2)); MS (EI, 70 eV): *m/z* (%) 220 (100) [M⁺], 138 (88) [M⁺ – C₆H₁₀], 137 (76) [M⁺ – C₆H₁₁], 123 (12) [M⁺ – C₆H₁₀ – CH₃], 122 (6) [M⁺ – C₆H₁₁ – CH₃], 106 (6), 83 (5); HRMS (70 eV): calcd for C₁₄H₂₀O₂: 220.1463, found: 220.1469.

(E)-2-(trans-Decahydro-1-naphthyl)bromoethene (23). To a suspension of bromomethyl(triphenyl)phosphonium bromide (3.5 g, 8.0 mmol) in 13 mL of dry THF at –78 °C was added KO^tBu (885 mg, 8.0 mmol). The yellow reaction mixture was stirred 30 min at this temperature after which a solution of *trans*-1-decalone (500 mg, 3.25 mmol) in 2.5 mL of THF was

added. The mixture was allowed to warm to room temperature, then stirred for 2 h, and diluted with water and ether. The aqueous solution was extracted with ether (3 × 20 mL). The combined organic layers were dried over Na₂SO₄ and evaporated under reduced pressure. The crude product was purified by flash chromatography on silica gel (95:5 hexane/EtOAc) to give 548 mg (73%) of pure **23** as a yellowish oil. *R_f*: 0.75 (9:1 hexane/EtOAc); ¹H NMR (250 MHz, CDCl₃): δ 5.76 (s, 1H, C=CHBr), 3.04–2.99 (m, 1H, H-2), 1.86–1.03 (m, 15H, decalin); ¹³C NMR (62.9 MHz, CDCl₃): δ 148.4 (C-1), 97.8 (C=CHBr), 48.8 (C-8a'), 44.6 (C-4a'), 34.4, 34.4, 32.6, 28.6 (C-2', C-4', C-5', C-8'), 26.6, 26.3, 26.2 (C-3', C-6', C-7'); MS (EI, 70 eV): *m/z* (%) 230/228 (13/14) [M⁺], 149 (100) [M⁺ – Br], 135 (8) [M⁺ – Br – CH₂], 107 (14), 96 (11); HRMS (70 eV): calcd for C₁₁H₁₇⁷⁹Br: 228.0514, found: 228.0516.

3-Methoxy-2-isopropoxyphenylboronic Acid (24). To a solution of aromatic compound **10** (1.20 g, 4.90 mmol) in 16 mL of THF at –78 °C was added dropwise *n*-BuLi (2.2 mL, 5.5 mmol) (2.5 M in hexane). The solution was slowly warmed to –40 °C, then cooled to –78 °C, and at this temperature B(OMe)₃ (2.4 mL, 25.2 mmol) was added. The mixture was warmed to room temperature and cooled to 0 °C, and 5% aqueous HCl was added until a pH of 6.5 was reached. The reaction mixture was diluted with 20 mL of ether and 20 mL of water and extracted with ether (3 × 20 mL). The combined organic layers were dried over Na₂SO₄ and evaporated under reduced pressure. The crude product was purified by flash chromatography on silica gel (4:1 hexane/EtOAc) to give 237 mg (23%) of pure **24** as a white solid. *R_f*: 0.36 (3:1 hexane/EtOAc); mp 81 °C; ¹H NMR (250 MHz, CDCl₃): δ 7.40 (dd, ³*J* = 7.2 Hz, ⁴*J* = 1.7 Hz, 1H, H-6), 7.13–7.00 (m, 2H, H-4, H-5), 6.25 (brs, 2H, OH), 4.84–4.69 (m, 1H, OCH(CH₃)₂), 3.86 (s, 3H, OCH₃), 1.31 (d, ³*J* = 6.2 Hz, 6H, OCH(CH₃)₂); ¹³C NMR (62.9 MHz, CDCl₃): δ 151.6 (C-3, C-2), 127.3 (C-6), 124.0 (C-5), 123.9 (C-1), 115.6 (C-4), 75.3 (OCH(CH₃)₂), 55.7 (OCH₃), 22.3 (OCH(CH₃)₂); MS (EI, 70 eV): *m/z* (%) 210 (28) [M⁺], 168 (70) [M⁺ – C(CH₃)₂], 167 (15) [M⁺ – CH(CH₃)₂], 150 (100) [M⁺ – H – OCH(CH₃)₂], 149 (27), 135 (12), 107 (10); HRMS (70 eV): calcd for C₁₀H₁₅O₄B: 210.1063; found: 210.1060.

3-[(1*E*)-(trans-Decahydro-1-naphthyl)methylene]-1-methoxy-2-isopropoxybenzene (25). To a solution of vinyl bromide **23** (77.8 mg, 0.340 mmol) in 1.1 mL of toluene was added Pd(PPh₃)₄ (10.6 mg, 9.19 μmol). The solution was stirred for 10 min, and a solution of boronic acid **24** (78.6 mg, 0.375 mmol) in 380 μL of ethanol and 228 μL of a 2 M solution of Na₂CO₃ were added. The solution was warmed to 90 °C for 24 h, diluted with ether and water, and extracted with ether (3 × 15 mL). The combined organic layers were dried over Na₂SO₄ and evaporated under reduced pressure. The crude product was purified by flash chromatography on silica gel (95:5 hexane/EtOAc) to give 93.7 mg (88%) of pure **25** as a colorless oil. *R_f*: 0.48 (9:1 hexane/EtOAc); ¹H NMR (500 MHz, CDCl₃): δ 6.97–6.94 (m, 1H, H-4), 6.78–6.73 (m, 2H, H-5, H-6), 6.17 (s, 1H, H-7), 4.30–4.25 (m, 1H, OCH(CH₃)₂), 3.85 (s, 3H, OCH₃), 2.84–2.81 (m, 1H, H-2'), 1.96–1.94 (m, 1H, H-2'), 1.87–0.84 (m, 14H, decalin), 1.24 (d, ³*J* = 6.2 Hz, 6H, OCH(CH₃)₂); ¹³C NMR (125.6 MHz, CDCl₃): δ 153.1 (C-1), 145.9 (C-2), 145.3 (C-1'), 134.3 (C-5), 122.8, 122.7 (C-1, C-4), 115.9 (C-7), 110.2 (C-6), 75.2 (OCH(CH₃)₂), 55.7 (OCH₃), 48.4 (C-8a'), 44.9 (C-4a'), 35.0, 34.7 (C-4', C-5'), 30.8, 29.1, (C-2', C-8'), 27.5, 26.6 (C-3', C-6', C-7'), 22.7, 22.2 (OCH(CH₃)₂); MS (EI, 70 eV): *m/z* (%) 314 (9) [M⁺], 242 (18), 226 (10), 200 (100), 185 (16), 135 (25), 130 (32); HRMS (70 eV): calcd for C₂₁H₃₀O₂: 314.2246, found: 314.2252.

6-[(1*E*)-(trans-Decahydro-1-naphthyl)methylene]-2-methoxyphenol (26). To a solution of compound **25** (86.6 mg, 0.292 mmol) in 6.3 mL of CH₂Cl₂ at 0 °C was added BCl₃ (1 M in CH₂Cl₂) (325 μL, 0.32 mmol). After the mixture was stirred at 0 °C for 1 h, water was added, and the mixture was extracted with CH₂Cl₂ (3 × 15 mL). The combined organic layers were dried over Na₂SO₄ and evaporated under reduced pressure. The crude product was purified by flash chromatography on silica gel (95:5 hexane/EtOAc) to give 73.9 mg (93%) of pure **26** as a colorless oil; *R_f*: 0.38 (9:1 hexane/EtOAc); ¹H

NMR (500 MHz, CDCl₃): δ 6.74–6.63 (m, 3H, H-3, H-4, H-5), 6.02 (s, 1H, H-7), 5.57 (d, ⁴*J* = 1.5 Hz, 1H, OH), 3.81 (s, 3H, OCH₃), 2.71–2.66 (m, 1H, H-2'), 1.94–1.05 (m, 15H, Decalin); ¹³C NMR (125.6 MHz, CDCl₃): δ 148.0 (C-2), 146.0 (C-1'), 143.0 (C-1), 125.4 (C-6), 122.8, (C-4), 118.9 (C-5), 113.5 (C-7), 108.7 (C-3), 55.9 (OCH₃), 48.4 (C-8a'), 45.0 (C-4a'), 35.0, 34.7 (C-4', C-5'), 31.0, 29.0, (C-2', C-8'), 27.7, 26.5, 26.3 (C-3', C-6', C-7'); MS (EI, 70 eV): *m/z* (%) 272 (42) [M⁺], 176 (10), 144 (7), 135 (100) [M⁺ – C₈O₂H₉], 93 (6); HRMS (70 eV): calcd for C₁₈H₂₄O₂: 272.1776, found: 272.1771.

3-[(trans-Decahydro-1-naphthyl)methyl]-1-methoxy-2-isopropoxybenzene (28). A solution of olefin **25** (129 mg, 0.411 mmol) in a 4:1 mixture of methanol–THF (9 mL) was hydrogenated for 48 h at room temperature and atmospheric pressure in the presence of 5% rhodium supported on alumina (27.0 mg, 0.132 mmol). The catalyst was filtered off, and the solvent was removed under reduced pressure. The crude product was purified by flash chromatography on silica gel (95:5 hexane/EtOAc) to give 122 mg (94%) of a 3:1 isomer mixture of **28** as a colorless oil; *R_f*: 0.58 (9:1 hexane/EtOAc); ¹H NMR (500 MHz, CDCl₃): δ 6.93–6.89 (m, 1H, H-4), 6.74–6.68 (m, 2H, H-5, H-6), 4.51–4.46 (m, 1H, OCH(CH₃)₂), 3.81 (s, 3H, OCH₃), 3.10 (dd, ²*J* = 13.0 Hz, ⁴*J* = 3.6 Hz, 1H, H-7), 2.72 (dd, ²*J* = 13.0 Hz, ⁴*J* = 3.7 Hz, 1H, H-7), 2.62–2.57 (m, 1H, H-1'), 2.17–2.14 (m, 1H, H-2'), 2.08–2.03 (m, 1H, H-2'), 1.93–0.81 (m, 14H, decalin), 1.29–1.25 (m, 6H, OCH(CH₃)₂); ¹³C NMR (125.6 MHz, CDCl₃): δ 152.8 (C-1), 145.1/145.0 (C-2), 137.2/136.6 (C-3), 123.0 (C-4), 122.8/122.6 (C-5), 109.5/109.4 (C-6), 74.2 (OCH(CH₃)₂), 55.5 (OCH₃), 48.5/46.8 (C-8a'), 43.1/43.0 (C-4a'), 39.2/36.3 (C-7), 35.2/35.0 (C-1'), 34.6/34.6, 32.2/31.2, 30.4 (C-4', C-5', C-8'), 28.9/27.2 (C-2'), 27.1/27.0, 26.7/26.6, 25.9 (C-3', C-6', C-7'), 22.8/22.6, 22.4/20.6 (OCH(CH₃)₂); MS (EI, 70 eV): *m/z* (%) = 316 (24) [M⁺], 274 (47) [M⁺ – C₃H₆], 254 (14), 222 (10), 206 (21), 180 (42), 149(30), 138 (67), 137 (100) [M⁺ – C₁₁O₂H₁₅], 95 (31), 81 (54); HRMS (70 eV): calcd for C₂₁H₃₂O₂: 316.2402, found: 316.2396.

N-(5-Benzyl-3,6-dioxo-4-N-L-serine-1,4-cyclohexadienyl)-L-serine (31a). A mixture of quinone **15** (15.0 mg, 65.8 μmol) and L-serine (10.2 mg, 97.1 μmol) in 7.8 mL of EtOH was stirred at 40 °C for 24 h in the presence of NaHCO₃ (22.2 mg, 0.264 mmol). After filtration, the filtrate was evaporated under reduced pressure, and the residue was purified by reversed-phase HPLC (VP 250/21 Nucleosil 100–7 C-18 HD, flow rate 13 mL/min; method A; UV detection at 300 nm; *t_R* 17.5 min) to afford **17a** (4.7 mg, 24%), as a dark red solid; [α]_D²⁰ = –23.5° (*c* = 0.085, MeOH), ¹H NMR (500 MHz, CD₃OD): 7.27–7.24 (m, 2H, H-2'(2)), 7.17–7.14 (m, 3H, H-3'(2), H-4), 5.39 (s, 1H, H-2), 4.48 (s, 1H, α-CH-4-Ser), 4.23 (s, 1H, α-CH-1-Ser), 4.02–3.94 (m, 3H, β-CH₂-4-Ser, β-CH-1-Ser), 3.86–3.81 (m, 2H, β-CH-1-Ser, H-7), 3.61 (d, ³*J* = 8.7 Hz, 1H, H-7); MS (ESI): *m/z*: calcd for C₁₉H₂₀N₂O₈: 404.37 found: 405 [M + H].

N-(5-Benzyl-3,6-dioxo-4-N-D-valine-1,4-cyclohexadienyl)-D-valine (31d). A mixture of quinone **15** (17.0 mg, 74.5 μmol) and D-valine (13.4 mg, 0.114 mmol) in 8.8 mL of EtOH was stirred at 30 °C for 24 h in the presence of NaHCO₃ (98 mg, 1.17 mmol). After filtration, the filtrate was evaporated under reduced pressure, and the residue was purified by reversed-phase HPLC (VP 250/21 Nucleosil 100–7 C-18 HD, flow rate 13 mL/min; method B, UV detection at 300 nm; *t_R* 4.2 min) to afford **31d** (18.4 mg, 75%), as a red solid; [α]_D²⁰ = +10.2° (*c* = 0.92, MeOH); ¹H NMR (500 MHz, CD₃OD): 7.30–7.12 (m, 5H, H-2'(2), H-3'(2), H-4'), 5.42 (s, 1H, H-2), 4.26–4.21 (m, 1H, α-CH-4-Val), 3.97 (d, ³*J* = 5.4 Hz, 1H, α-CH-1-Val), 3.80 (s, 2H, H-7), 2.34–2.27 (m, 2H, β-CH-Val), 1.01 (d, ³*J* = 6.9 Hz, 3H, γ-CH₃-4-Val), 0.98 (d, ³*J* = 6.9 Hz, 3H, γ-CH₃-4-Val), 0.77 (d, ³*J* = 6.9 Hz, 3H, γ-CH₃-1-Val), 0.71 (d, ³*J* = 6.9 Hz, 3H, γ-CH₃-1-Val); MS (ESI): *m/z*: calcd for C₂₃H₂₈N₂O₆: 428.48 found: 429 [M + H].

2-Isopropoxyphenol (40). To 270 mL of DMSO was added KOH (28.3 g, 0.505 mol). After the mixture was stirred for 10 min catechol **39** (15.0 g, 0.136 mol) was added, followed after 10 min by 2-bromopropane (12.8 mL, 0.136 mol). Stirring was continued for 30 min after which the KOH was filtered, and

the filtrate was diluted with 200 mL of CH_2Cl_2 . The organic layer was washed with saturated solution of NH_4Cl ($2 \times$) and NaCl ($2 \times$), dried over Na_2SO_4 , and evaporated under reduced pressure. The crude product was purified by flash chromatography on silica gel (95:5 hexane/EtOAc) to give 11.0 g (53%) of pure **7** as a colorless oil. R_f : 0.42 (9:1 hexane/EtOAc); ^1H NMR (250 MHz, CDCl_3): δ 6.95–6.91 (m, 1H, H-4), 6.87–6.78 (m, 3H, H-3, H-5, H-6), 5.81 (brs, 1H, OH), 4.59–4.50 (m, 1H, $\text{OCH}(\text{CH}_3)_2$), 1.34 (d, $^3J = 6.1$ Hz, 6H, $\text{OCH}(\text{CH}_3)_2$); ^{13}C NMR (62.9 MHz, CDCl_3): δ 146.6 (C-2), 144.6 (C-1), 121.4 (C-4), 120.0 (C-5), 114.6 (C-6), 113.4 (C-3), 71.5 ($\text{OCH}(\text{CH}_3)_2$), 22.1 ($\text{OCH}(\text{CH}_3)_2$); MS (EI, 70 eV): m/z (%) 152 (13) [M^+], 110 (100) [$\text{M}^+ - \text{C}(\text{CH}_3)_2$]; HRMS (70 eV): calcd for $\text{C}_9\text{H}_{12}\text{O}_2$: 152.0837, found: 152.0846.

2-Hydroxy-3-isopropoxyphenyl Bromide (41). Br_2 (3.66 mL, 71.3 mmol) was added dropwise to a solution of *tert*-butylamine (15.3 mL, 72.7 mmol) in 134 mL of dry toluene at -30°C . After being stirred for 0.5 h, the reaction mixture was cooled to -60°C . A solution of 2-isopropoxyphenol **40** (11.0 g, 72.3 mol) in 9 mL of CH_2Cl_2 was added dropwise to the reaction mixture, and the mixture was warmed to room temperature over a period of 5 h. The reaction mixture was treated with 10% $\text{Na}_2\text{S}_2\text{O}_3$, washed with brine, and dried over Na_2SO_4 . The crude product was purified by flash chromatography on silica gel (95:5 hexane/EtOAc) to give 6.5 g (39%) of pure **41** as a colorless oil. R_f : 0.63 (3:1 hexane/EtOAc); ^1H NMR (250 MHz, CDCl_3): δ 7.06 (dd, $^3J = 8.1$ Hz, $^4J = 1.3$ Hz, 1H, H-6), 6.79 (dd, $^3J = 8.1$ Hz, $^4J = 1.2$ Hz, 1H, H-4), 6.70 (*ψ*t, $^3J = 8.1$ Hz, 1H, H-5), 6.02 (s, 1H, OH), 4.59–4.53 (m, 1H, $\text{OCH}(\text{CH}_3)_2$), 1.36 (d, $^3J = 6.1$ Hz, 6H, $\text{OCH}(\text{CH}_3)_2$); ^{13}C NMR (62.9 MHz, CDCl_3): δ 145.3 (C-3), 144.2 (C-2), 124.8 (C-6), 120.5 (C-5), 112.4 (C-4), 108.3 (C-1), 72.3 ($\text{OCH}(\text{CH}_3)_2$), 22.1 ($\text{OCH}(\text{CH}_3)_2$); MS (EI, 70 eV): m/z (%) 232/230 (21/22) [M^+], 190/188 (97/100) [$\text{M}^+ - \text{C}(\text{CH}_3)_2$], 108 (5); HRMS (70 eV): calcd for $\text{C}_9\text{H}_{11}\text{O}_2^{81}\text{Br}$: 231.9922, found: 231.9920.

2-Bromo-6-isopropoxy-*p*-benzoquinone (42). To a solution of 2-hydroxy-3-isopropoxyphenyl bromide **8** (5.0 g, 22.0 mmol) in 138 mL of DMF was added 80.6 mg (0.24 mmol) of salcomine (*N,N*-bis(salicylidene)ethylendiamine cobalt(II) salt hydrate). The solution was stirred at room temperature under an oxygen atmosphere for 16 h, diluted with 200 mL of ether and 100 mL of water, and extracted with ether (3×150 mL). The combined organic layers were dried over Na_2SO_4 and evaporated under reduced pressure. The crude product was purified by flash chromatography on silica gel (9:1 hexane/EtOAc) to give 3.9 g (73%) of pure **42** as a yellow oil. R_f : 0.47 (3:1 hexane/EtOAc); ^1H NMR (250 MHz, CDCl_3): δ 7.19 (d, $^4J = 2.1$ Hz, 1H, H-3), 5.93 (d, $^4J = 2.1$ Hz, 1H, H-5), 4.58–4.48 (m, 1H, $\text{OCH}(\text{CH}_3)_2$), 1.36 (d, $^3J = 6.1$ Hz, 6H, $\text{OCH}(\text{CH}_3)_2$); ^{13}C NMR (62.9 MHz, CDCl_3): δ 184.7 (C-1), 174.5 (C-4), 162.3 (C-6), 138.0 (C-3), 126.5 (C-2), 107.8 (C-5), 72.5 ($\text{OCH}(\text{CH}_3)_2$), 21.7 ($\text{OCH}(\text{CH}_3)_2$); MS (EI, 70 eV): m/z (%) 246/244 (3/3) [M^+], 232/230 (19/20), 190/188 (97/100), 108 (5), 79 (5); HRMS (70 eV): calcd for $\text{C}_9\text{H}_9\text{O}_3^{79}\text{Br}$: 243.9735, found: 243.9741.

2,5-Dimethoxy-3-isopropoxyphenyl Bromide (43). To a suspension of 2-bromo-6-isopropoxy-*p*-benzoquinone **42** (3.9 g, 16.1 mmol) in 42 mL of ethanol at 0°C was added NaBH_4 (1.7 g, 45.4 mmol) in portions. After addition was complete, the reaction mixture was allowed to stir for 4 h at 0°C . The excess of NaBH_4 was destroyed by careful addition of 1 M HCl. The reaction mixture was diluted with 20 mL of water and 50 mL of ether and extracted with ether (2×50 mL). The combined organic layers were washed with water (2×30 mL), dried over Na_2SO_4 , and evaporated under reduced pressure to give 3.3 g of the hydroquinone, which was subjected to the *O*-methylation without further purification.

To a stirred mixture of 2-bromo-6-isopropoxyhydroquinone (3.3 g) in 6 mL of ethanol, dimethyl sulfate (8.25 mL, 86.5 mmol), and NaHSO_3 (0.23 g, 2.18 mmol) at 0°C was added a solution of NaOH (3.3 g, 82.5 mmol) in 18.5 mL of water over 30 min. The mixture was warmed to 70 – 80°C for 4 h and diluted with water and ether. The aqueous solution was extracted with ether (3×80 mL). The combined organic layers were washed with 2 N NaOH (2×200 mL) and water ($2 \times$

200 mL), dried over MgSO_4 , and evaporated under reduced pressure. The crude product was purified by flash chromatography on silica gel (95:5 hexane/EtOAc) to give 2.9 g (66%, two steps) of pure **43** as a colorless oil. R_f : 0.44 (9:1 hexane/EtOAc); ^1H NMR (250 MHz, CDCl_3): δ 6.61 (d, $^4J = 2.8$ Hz, 1H, H-6), 6.41 (d, $^4J = 2.8$ Hz, 1H, H-4), 4.56–4.50 (m, 1H, $\text{OCH}(\text{CH}_3)_2$), 3.77 (s, 3H, C5– OCH_3), 3.72 (s, 3H, C2– OCH_3), 1.34 (d, $^3J = 6.1$ Hz, 6H, $\text{CH}(\text{CH}_3)_2$); ^{13}C NMR (62.9 MHz, CDCl_3): δ 156.2 (C-5), 152.2 (C-3), 141.9 (C-2), 117.6 (C-1), 108.4 (C-6), 103.0 (C-4), 71.5 ($\text{OCH}(\text{CH}_3)_2$), 60.4 (C-5– OCH_3), 55.6 (C-2– OCH_3), 21.9 ($\text{OCH}(\text{CH}_3)_2$); MS (EI, 70 eV): m/z (%) 276/274 (41/42) [M^+], 246/244 (20/20) [$\text{M}^+ - 2\text{CH}_3$], 234/232 (49/50) [$\text{M}^+ - \text{C}(\text{CH}_3)_2$], 219/217 (97/100), 204/202 (64/65) [$\text{M}^+ - \text{C}(\text{CH}_3)_2 - 2\text{CH}_3$], 191 (12), 189/187 (49/38), 154 (7), 139 (11); HRMS (70 eV): calcd for $\text{C}_{11}\text{H}_{15}\text{O}_3^{79}\text{Br}$: 274.0205, found: 274.0199.

6-Benzyl-1,4-dimethoxy-2-isopropoxybenzene (45). To a solution of 2,5-dimethoxy-3-isopropoxyphenyl bromide **43** (200 mg, 0.728 mmol) in 1.9 mL of THF at -78°C was added dropwise *n*-BuLi (2.5 M in hexane) (320 μL , 0.8 mmol). After the mixture was stirred at this temperature for 30 min, CuI (169 mg, 0.887 mmol) was added. The solution was slowly warmed to -40°C , then cooled to -78°C , and a solution of benzyl bromide (115 μL , 0.97 mmol) in 0.6 mL of THF was added. The mixture was warmed to room temperature, diluted with 20 mL of ether and 20 mL of water, and extracted with ether (1×20 mL). The combined organic layers were washed with a saturated solution of Na_2CO_3 until the aqueous layer was not blue, dried over Na_2SO_4 , and evaporated under reduced pressure. The crude product was purified by flash chromatography on silica gel (95:5 hexane/EtOAc) to give 114 mg (55%) of **45** as a colorless oil; ^1H NMR (250 MHz, CDCl_3): δ 7.27–7.16 (m, 5H, H-2'(2), H-3'(2), H-4'), 6.37 (d, $^4J = 2.8$ Hz, 1H, H-5), 6.23 (d, $^4J = 3.0$ Hz, 1H, H-3), 4.56–4.46 (m, 1H, $\text{OCH}(\text{CH}_3)_2$), 3.95 (s, 2H, H-7), 3.70 (s, 3H, C-1– OCH_3), 3.66 (s, 3H, C-4– OCH_3), 1.36 (d, $^3J = 6.1$ Hz, 6H, $\text{OCH}(\text{CH}_3)_2$); ^{13}C NMR (62.9 MHz, CDCl_3): δ 155.6 (C-4), 151.5 (C-2), 141.0 (C-1'), 135.2 (C-1), 128.9, 128.6, 128.6 (C-6, C-2'(2), C-3'(2)), 125.9 (C-4'), 106.5 (C-5), 101.0 (C-3), 70.7 ($\text{OCH}(\text{CH}_3)_2$), 60.4 (C-1– OCH_3), 55.4 (C-4– OCH_3), 36.2 (C-7), 22.1 ($\text{OCH}(\text{CH}_3)_2$); MS (EI, 70 eV): m/z (%) 286 (93) [M^+], 244 (87) [$\text{M}^+ - \text{C}_6\text{H}_5$], 229 (100) [$\text{M}^+ - \text{C}_4\text{H}_9$], 183 (9), 153 (8), 141 (8), 91 (16); HRMS (70 eV): calcd for $\text{C}_{18}\text{H}_{22}\text{O}_3$: 286.1569, found: 286.1573.

3-Benzyl-2,5-dimethoxy-2,5-cyclohexadiene-1,4-dione (47). To a solution of Fremy's salt ($\text{ON}(\text{SO}_3\text{K})_2$, 77.4 mg, 0.289 mmol) in 1.8 mL of Na_2CO_3 (15% solution in water) were added Aliquat 336 (tricaprylmethylammonium chloride) (51.6 mg) in 710 μL benzene and phenol **46** (30.0 mg, 0.115 mmol) in 1.4 mL of benzene. The reaction mixture was stirred at room temperature for 3 h and diluted with ether and water. The water layer was extracted with ether (3×10 mL). The combined organic layers were dried over Na_2SO_4 and evaporated under reduced pressure. The crude product was purified by flash chromatography on silica gel (5:1 hexane/EtOAc) to give 27.4 mg (92%) of **47** as a yellow oil; R_f : 0.22 (3:1 hexane/EtOAc); ^1H NMR (250 MHz, CDCl_3): δ 7.26–7.15 (m, 5H, H-2'(2), H-3'(2), H-4'), 5.71 (s, 1H, H-6), 4.08 (s, 3H, C-2– OCH_3), 3.79 (s, 3H, C-5– OCH_3), 3.77 (s, 2H, H-7); ^{13}C NMR (62.9 MHz, CDCl_3): δ 183.6 (C-4), 181.9 (C-1), 158.7 (C-5), 155.7 (C-2), 138.9 (C-1'), 129.0, 128.5, 128.4 (C-2'(2), C-3'(2), C-4'), 126.3 (C-1), 105.4 (C-6), 61.3 (C-5– OCH_3), 56.4 (C-2– OCH_3), 28.7 (C-7); MS (EI, 70 eV): m/z (%) 258 (45) [M^+], 227 (100) [$\text{M}^+ - \text{OCH}_3$], 215 (66), 197 (5), 183 (10), 167 (6), 115 (14), 91 (51); HRMS (70 eV): calcd for $\text{C}_{15}\text{H}_{14}\text{O}_4$: 258.0892, found: 258.0896.

3-Benzyl-2-hydroxy-5-methoxy-2,5-cyclohexadiene-1,4-dione (48) To a solution of quinone **47** (27.4 mg, 0.106 mmol) in 5.8 mL of MeOH and 3.4 mL of H_2O was added water until the starting material was dissolved. To the reaction mixture was added 9 drops of 1 N KOH, and the dark red solution was stirred at room temperature for 12 h. The reaction mixture was diluted with water and ether, and solid NH_4Cl was added. The aqueous solution was extracted with ether until decolorization. The combined organic layers were dried over Na_2SO_4 and evaporated under reduced pressure. The crude product

was purified by flash chromatography on silica gel (100:1 CHCl₃/MeOH) to give 17.6 mg (68%) of **48** as a yellow solid (during the contact with silicagel compound **48** turns purple). *R*_f: 0.06 (3:1 hexane/EtOAc); mp 116 °C; ¹H NMR (250 MHz, CDCl₃): δ 7.36–7.16 (m, 5H, H-2'(2), H-3'(2), H-4'), 5.83 (s, 1H, H-6), 3.82 (s, 3H, C-5-OCH₃), 3.78 (s, 2H, H-7); ¹³C NMR (62.9 MHz, CDCl₃): δ 182.7 (C-4), 181.5 (C-1), 161.8 (C-5), 151.4 (C-2), 138.6 (C-1'), 129.0, 128.3, (C-2'(2), C-3'(2)), 126.2 (C-4'), 117.8 (C-3), 102.2 (C-6), 56.7 (C-5-OCH₃), 28.3 (C-7); MS (EI, 70 eV): *m/z* (%) 244 (100) [M⁺], 243 (42) [M⁺ - H], 229 (9) [M⁺ - CH₃], 215 (10), 183 (23), 131 (8), 167 (6), 103 (5), 91 (29); HRMS (70 eV): calcd for C₁₄H₁₂O₄: 244.0736, found: 244.0733.

Tyrosine Kinase Assay. The catalytic sections of the corresponding tyrosine kinases were expressed as GST fusion proteins (Klinik für Tumorbiologie, Freiburg, Germany).

In brief, the assays were performed in white 96 well microtiter plates (Greiner) which had been coated at 4 °C for 16 h with 12.5 μg polyGlu-Tyr 4:1 sodium salt (Sigma) in 125 μL of PBS (phosphate buffered saline, Gibco) per well. The coating solution was flicked off and the plates were washed twice with PBST (PBS + 0.5% Tween-20). Kinases were diluted in kinase buffer (100 mM HEPES pH 7.4, 100 mM NaCl) and added at 20 ng protein in 50 μL of buffer. Stock solutions of the test compounds were made in DMSO and diluted to a final concentration of 5% DMSO with water (working solution). Twenty five microliters of the working solutions was added to each well. The kinase reaction was started by addition of 25 μL of ATP (100 μM in 40 mM MnCl₂) using a multichannel pipet. Negative controls received 40 mM MnCl₂ without ATP. The plates were incubated at RT for 30 min. The microtiter plates were washed three times with PBST. One hundred microliters of anti phosphotyrosine antibody (PY20, Calbiochem) conjugated to horseradish peroxidase (POD) was added at 1:5000 dilution in PBST + 0.1% BSA (bovine serum albumin, Calbiochem) and incubated for 1 h at RT. Plates were washed five times with PBST. For detection, 100 μL of POD chemiluminescence substrate (Roche) was added. The resulting light emission was detected with an Orion luminescence reader (Berthold).

Acknowledgment. This research was supported by the Fonds der Chemischen Industrie. L.K. wishes to acknowledge the support by the Studienstiftung des deutschen Volkes (Promotionsstipendium), the Fonds der Chemischen Industrie (Kekule-Stipendium), and e-fellows.net (Online-Stipendium). R.M. is grateful to the Land Baden-Württemberg for a scholarship from the Landesgraduierföderung.

Supporting Information Available: Further experimental details are available free of charge via the Internet at <http://pubs.acs.org>.

References

- Hubbard, S. R.; Till, J. H. Protein Tyrosine Kinases: Structure and Function. *Annu. Rev. Biochem.* **2000**, *69*, 373–98.
- Yancopoulos, G. D.; Davis, S.; Gale, N. W.; Rudge, J. S.; Wiegand, S. J.; Holash, J. Vascular-specific growth factors and blood vessel formation. *Nature* **2000**, *407*, 242–248.
- Hiratsuka, S.; Maru, Y.; Okada, A.; Seiki, M.; Noda, T.; Shibuya, M. Involvement of Flt-1 tyrosine kinase (vascular endothelial growth factor receptor-1) in pathological angiogenesis. *Cancer Res.* **2001**, *61*, 1207–1213.
- Kubo, H.; Fujiwara, T.; Jussila, L.; Hashi, H.; Ogawa, M.; Shimizu, K.; Awane, M.; Sakai, Y.; Takabayashi, A.; Alitalo, K.; Yamaoka, Y.; Nishikawa, S. I. Involvement of vascular endothelial growth factor receptor-3 in maintenance of integrity of endothelial cell lining during tumor angiogenesis. *Blood* **2000**, *96*, 546–553.
- Stratmann, A.; Acker, T.; Burger, A. M.; Amann, K.; Risau, W.; Plate, K. H. Differential inhibition of tumor angiogenesis by TIE2 and vascular endothelial growth factor receptor-2 dominant-negative receptor mutants. *Int. J. Cancer* **2001**, *91*, 273–282.
- Stacker, S. A.; Caesar, C.; Baldwin, M. E.; Thornton, G. E.; Williams, R. A.; Prevo, R.; Jackson, D. G.; Nishikawa, S.; Kubo, H.; Achen, M. G. VEGF-D promotes the metastatic spread of tumor cells via the lymphatics. *Nat. Med.* **2001**, *7*, 186–191.
- Skobe, M.; Hawighorst, T.; Jackson, D. G.; Prevo, R.; Janes, L.; Velasco, P.; Riccardi, L.; Alitalo, K.; Claffey, K.; Detmar, M.; Induction of tumor lymphangiogenesis by VEGF-C promotes breast cancer metastasis. *Nat. Med.* **2001**, *7*, 192–198.
- Giannis, A.; Rüssam, F. Integrin antagonists and other low molecular weight compounds as inhibitors of angiogenesis: New drugs in cancer therapy. *Angew. Chem.* **1997**, *109*, 606–609; *Angew. Chem., Int. Ed. Engl.* **1997**, *36*, 588–590 and refs therein.
- Carmeliet, P.; Jain, R. K. Angiogenesis in cancer and other diseases. *Nature* **2000**, *407*, 249–257 and refs therein.
- O'Connor, R.; Fennely, C.; Krause, D. Regulation of survival signals from the insulin-like growth factor-I receptor. *Biochem. Soc. Trans.* **2000**, *28*, 47–51.
- Hudziak, R. M.; Ullrich, A. Cell transformation potential of a HER2 transmembrane domain deletion mutant retained in the endoplasmic reticulum. *J. Biol. Chem.* **1991**, *266*, 24109–24115.
- Heidin, C.-H.; Rönstrand, L. Growth factor receptor in cell transformation. In *Oncogenes and Tumor Suppressors*; Peters, G., Vousden, K., Eds.; Oxford University Press, Cary, NC, 1997; pp 55–85.
- Cohen, P. Protein kinases- the major drug targets of the twenty-first century? *Nat. Rev. Cancer* **2002**, *1*, 309–315.
- Bridges, A. J. Chemical Inhibitors of Protein Kinases. *Chem. Rev.* **2001**, *101*, 2541–2571.
- Breinbauer, R.; Vetter, I.; Waldmann, H. From Protein Domains to Drug Candidates – Natural Products as Guiding Principles in the Design and Synthesis of Compound Libraries. *Angew. Chem., Int. Ed.* **2002**, *41*, 2878–2890.
- Part of this work was published in preliminary form: Stahl, P.; Kissau, L.; Mazitschek, R.; Giannis, A.; Waldmann, H. Natural Product Derived Receptor Tyrosine Kinase Inhibitors: Identification of IGF1R, Tie-2 and VEGFR-3 Inhibitors. *Angew. Chem., Int. Ed.* **2002**, *41*, 1174–1178.
- Kobayashi, J.; Madono, T.; Shigemori, H. Nakijiquinones C and D, New Sesquiterpenoid Quinones with a Hydroxy Amino Acid Residue from a Marine Sponge Inhibiting c-erbB-2 Kinase. *Tetrahedron* **1995**, *51*, 10867–10874.
- Stahl, P.; Kissau, L.; Mazitschek, R.; Huwe, A.; Furet, P.; Giannis, A.; Waldmann, H. Total Synthesis and Biological Evaluation of the Nakijiquinones. *J. Am. Chem. Soc.* **2001**, *123*, 11586–11593.
- See e. g. Bold, G.; Altmann, K.-H.; Frei, J.; Marc, L.; Manley, P. W.; Traxler, P.; Wietfeld, B.; Brüggem, J.; Buchdunger, E.; Cozens, R.; Ferrari, S.; Furet, P.; Hofmann, F.; Martiny-Baron, G.; Mestan, J.; Rösler, J.; Sills, M.; Stover, D.; Acemoglu, F.; Boss, E.; Emmenegger, R.; Lässer, L.; Masso, E.; Roth, R.; Schlachter, C.; Vetterli, W.; Wyss, D.; Wood, J. M. New Anilinothalazines as Potent and Orally Well Absorbed Inhibitors of the VEGF Receptor Tyrosine Kinases Useful as Antagonists of Tumor-Driven Angiogenesis. *J. Med. Chem.* **2000**, *43*, 2310–2323 and refs therein.
- Ishizaki, M.; Ozaki, K.; Kanematsu, A.; Isoda, T. Hoshino, Synthetic approaches toward spiro[2,3-dihydro-4H-1-benzopyran-4,1'-cyclohexan]-2-one derivatives via radical reactions: total synthesis of (±)-lycoramine. *O. J. Org. Chem.* **1993**, *58*, 3877–3885.
- Wakamatsu, T.; Nishi, T.; Ohnuma, T.; Ban, Y. A convenient synthesis of juglone via neutral salcomine oxidation. *Synth. Commun.* **1984**, *14*, 1167–1173.
- Miyaura, N.; Suzuki, A. Palladium-Catalyzed Cross-Coupling Reactions of Organoboron Compounds. *Chem. Rev.* **1995**, *95*, 2457–2483.
- Dolan, S. C.; Millan, J. M. A New Method for the Deoxygenation of Tertiary and Secondary Alcohols. *J. Chem. Soc., Chem. Commun.* **1985**, *22*, 1588–1589.
- Genot, A.; Florent, J.-C.; Monneret, C. Anthracyclinone. 3. Chiral pool synthesis of anthracyclinones via tetralin intermediates. *J. Org. Chem.* **1987**, *52*, 1057–1063.
- Takai, K.; Nitta, K.; Utimoto, K. Simple and selective method for aldehydes (RCHO) fudarw. (E)-haloalkenes (RCH: CHX) conversion by means of a haloform-chromous chloride system. *J. Am. Chem. Soc.* **1986**, *108*, 7408–7410.
- Harada, T.; Katsuhira, T.; Hattori, K.; Oku, A. Stereochemistry in carbenoid formation by bromine/lithium and bromine/zinc exchange reactions of gem-dibromo compounds. *Tetrahedron* **1994**, *50*, 7987–8002.
- Kaufman, T. S. Synthesis and mass spectral data of four potential biomarkers related to the C19 tricyclanes found Australian oils and puget sound sediments. *Synth. Commun.* **1995**, *25*, 1205–1221.
- See ref 1 and refs cited therein.
- Olson, G. L.; Cheung, H.-C.; Morgan, K.; Saucy, G. A new synthesis of alpha-tocopherol. *J. Org. Chem.* **1980**, *45*, 803–805.
- A homology model of the ATP binding site of KDR has been used to evaluate the anilinothalazine-class of RTK Inhibitors. See ref 18.

- (31) PDB entries 1FGI and 2FGI
- (32) Marti-Renom, M. A.; Stuart, A. C.; Fiser, A.; Sanchez, R.; Melo, F.; Sali, A. Comparative Protein Structure Modeling of Genes and Genomes. *Annu. Rev. Biophys. Biomol. Struct.* **2000**, *29*, 291–325.
- (33) This assumption would have also permitted the choice of the IGF1R or IRK structure as a templates. Indeed, this possibility was exploited, and the resulting 3D models were also used in the evaluation of the nakijiquinone analogues. However, the sequence homology to the VEGFs and Tie-2 is lower.
- (34) Davis, A. M.; Teague, S. J. Hydrogen Bonding, Hydrophobic Interactions, and Failure of the Rigid Receptor Hypothesis. *Angew. Chem., Int. Ed.* **1999**, *38*, 736–749.
- (35) Mohammadi, M.; McMahon, G.; Sun, L.; Tang, C.; Hirth, P.; Yeh, B. K.; Hubbard, S. R.; Schlessinger, J. Structure of the Tyrosine Kinase Domain of Fibroblast Growth Receptor in Complex with Inhibitors. *Science* **1997**, *276*, 955–960.
- (36) Morgenstern, B. Improvement of the segment-to-segment approach to multiple sequence alignment. *Bioinformatics* **1999**, *15*, 211–218.
- (37) Sali, A.; Potterton, L.; Yuan, F.; van Vlijmen, H.; Karplus, M. Evaluation of Comparative Protein Modeling by MODELLER. *Proteins* **1995**, *23*, 318–326.
- (38) Modeller 4.0 Manual. For additional references and information please refer to Sali@rockvax.rockefeller.edu.
- (39) Hoft, R. W. W.; Vriend, G.; Sander, C.; Abola, E. E. Errors in protein structure. *Nature* **1996**, *381*, 272.
- (40) WitnotP is a molecular modeling software developed by and licensed from Novartis AG, Basel, Switzerland. For further information and licensing conditions please contact Dr. Armin Widmer at Novartis AG.
- (41) Brooks, B. R.; Brucoleri, R. E.; Olafson, B. D.; States, D. J.; Swaminathan, S.; Karplus, M. CHARMM: A Program for Macromolecular Energy, Minimization, and Dynamics Calculations. *J. Comput. Chem* **1983**, *4*, 187–217.
- (42) For a detailed description of how this figure was created, see Experimental Section.
- (43) Knighton, D. R.; Zheng, J. H.; Ten Eyck, L. F.; Ashford, V. A.; Xuong, N. H.; Taylor, S. S.; Sowadski, J. M. Crystal Structure of the Catalytic Subunit of Cyclic Adenosine Monophosphate-Dependent Protein Kinase. *Science* **1991**, *253*, 407–414.
- (44) Arnold, L. D.; Calderwood, D. J.; Dixon, R. W.; Johnston, D. N.; Kamens, J. S.; Munschauer, R.; Rafferty, P.; Ratnofsky, S. E. Pyrrolo[2,3-*d*]pyrimidines Containing an Extended 5-Substituent as Potent and Selective Inhibitors of lck I. *Bioorg. Med. Chem. Lett.* **2000**, *10*, 2167–2170.
- (45) Burchat, A. F.; Calderwood, D. J.; Hirst, G. C.; Holman, N. J.; Johnston, D. N.; Munschauer, R.; Rafferty, P.; Tometzki, G. B. Pyrrolo[2,3-*d*]pyrimidines Containing an Extended 5-Substituent as Potent and Selective Inhibitors of lck. *Bioorg. Med. Chem. Lett.* **2000**, *10*, 2171–2174.
- (46) Calderwood, D. J.; Johnston, D. N.; Munschauer, R.; Rafferty, P. Pyrrolo[2,3-*d*]pyrimidines Containing Diverse N-7 Substituents as Potent Inhibitors of Lck. *Bioorg. Med. Chem. Lett.* **2002**, *12*, 1683–1686.
- (47) Burchat, A. F.; Calderwood, D. J.; Friedman, M. M.; Hirst, G. C.; Li, B.; Rafferty, P.; Ritter, K.; Skinner, B. S. Pyrazolo[3,4-*d*]pyrimidines Containing an Extended 3-Substituent as Potent Inhibitors of Lck – a Selective Insight. *Bioorg. Med. Chem. Lett.* **2002**, *12*, 1687–1690.
- (48) Stieber, F.; Mazitschek, R.; Soric, N.; Giannis, A.; Waldmann, H. Traceless Solid-Phase Synthesis of 2-Aminothiazoles: Receptor Tyrosine Kinase Inhibitors with Dual Selectivity for Tie-2 and VEGFR-2. *Angew. Chem., Int. Ed.* **2002**, *41*, 4757–4761.
- (49) Zhou, B.-N.; Johnson, R. K.; Mattern, M. R.; Fisher, P. W.; Kingston, D. G. I.; The First Naturally Occurring Tie 2 Inhibitor. *Org. Lett.* **2001**, *3*, 4047–4049.
- (50) A homology model of the IGF1R kinase domain was also created. The conclusions drawn with respect to the binding modes of the nakijiquinone analogues were essentially the same as those derived from the available crystal structures.
- (51) McTigue, M. A.; Wickersham, J. A.; Pinko, C.; Showalter, R. E.; Parast, C. V.; Tempczyk-Russell, A.; Gehring, M. R.; Mroczkowski, B.; Kan, C.-C.; Villafranca, J. E.; Appelt, K. Crystal structure of the kinase domain of human vascular endothelial growth factor receptor 2: a key enzyme in angiogenesis. *Structure* **1999**, *7*, 319–330.

JM0307943